Tantalum – Carbon Functionalities Bonded to a Calix[4]arene-Oxo Matrix: The Chemistry of Mono-, Dialkyl, and Butadiene Derivatives of Tantalum(V)

Barbara Castellano,[a] Euro Solari,[a] Carlo Floriani,*[a] Nazzareno Re,[b] Angiola Chiesi-Villa,[c] and Corrado Rizzoli[c]

Abstract: The synthesis of the starting compounds [Ta_2{μ-*p*-*t*Bu-calix[4]-$(O)_4$}$_2Cl_2$] (**3**) and [Ta{*p*-*t*Bu-calix[4]-(OMe)$(O)_3$}Cl_2] (**4**) for our investigations of calix[4]arene – tantalum organometallic chemistry has been achieved by the reaction of $TaCl_5$ with *p*-*t*Bu-calix[4]-$(OH)_4$ (**1**) and *p*-*t*Bu-calix[4]-$(OMe)_2$-$(OH)_2$ (**2**), whereby the latter compound underwent an acid-assisted demethylation. The alkylation of **3** by standard procedures led to the dimeric [Ta_2{μ-*p*-*t*Bu-calix[4]-$(O)_4$}$_2R_2$] derivatives (R = alkyl or aryl), which are in equilibrium with the corresponding monomeric forms in solution. An alternative route to these complexes is the pyridine-assisted demethylation of [Ta{*p*-*t*Bu-calix[4]-(OMe)$(O)_3$}R_2], which is obtained from the alkylation of **4**. The latter complexes, unlike [Ta_2{μ-*p*-*t*Bu-calix[4]-$(O)_4$}$_2R_2$], undergo migratory insertion reactions with CO and *t*BuNC to give the corresponding η^2-ketones and η^2-imines. Both classes of compounds undergo a pyridine-induced demethylation. The bis(allyl) derivative [Ta{*p*-*t*Bu-calix[4]-(OMe)$(O)_3$}$(\eta^3$-allyl$)_2$] undergoes a double migratory insertion reaction of the allyl groups to give the corresponding η^2-ketone and η^2-imine, respectively, in the reactions with CO and *t*BuNC. Although butadiene is π^2,η^4-bonded to the metal, the tantalum – butadiene fragment in [Ta{*p*-*t*Bu-calix[4]-(OMe)$(O)_3$}$(\eta^4$-$C_4H_6)$] (**25**) behaves as if it were η^4,σ^2-π bonded in the migratory insertion reaction with *t*BuNC and Me_2CO. In the reaction with PhN_3, complex **25** behaves as a source of d^2-tantalum(III) and leads to the nitrene derivative **28**.

Keywords: butadiene · calix[4]arene · migratory insertion reactions · tantalum · unsaturated ligands

Introduction

Calix[4]arenes[1] can be used in organometallic chemistry as a preorganized set of O_4 donor atoms with a number of distinctive peculiarities versus four independent phenoxo groups.[2] The coordination environment is largely governed by the set of four oxygen atoms attached to the calix[4]arene skeleton in a quasiplanar arrangement with the axial coordination site inside the cavity very rarely or almost inaccessible. We can tune both the overall charge of the macrocycle and the strength of the metal – oxygen interactions by partial methylation of the phenoxo groups. The resulting ether group, which would never act as a monodentate ligand, is kept close to the metal by a macrocyclic effect and can function as a spectator ligand, weakly interacting with the metal when necessary, or even able to provide an additional coordination site. The metal – calix[4]arene fragment has a particularly attractive diversity compared to the very well-known [Cp_2M] fragment.[3] It can engage four frontier orbitals, three of which are more accessible. In addition, the three orbitals have a facial arrangement in contrast to the meridional arrangement found in the [Cp_2M] complexes.[2d, 2e] We would also emphasize that the calix[4]arene fragment acts as a spectroscopic probe in the ^{1}H NMR spectrum with the differentiation of the *t*Bu substituents and, mainly, with the bridging methylenes behaving as heterotopic hydrogens in the structure rigidified by the metalation. These hydrogens appear as a pair of doublets, whose separation is somehow related to the coordination number of the metal, and which are very sensitive to the symmetry of the substrate bound to the metal. This report deals with the organometallic chemistry of tantalum(V) anchored to the tetraoxo matrix, as defined by either the calix[4]arene tetraanion (***A***) or the monomethoxycalix[4]arene trianion (***B***). In particular, we describe the synthesis and the chemical reactivity of tantalum σ- and π-bonded to organic fragments, including the base-induced demethylation of the methoxycalix[4]arene. This reaction

[a] Prof. Dr. C. Floriani, Dr. E. Solari, B. Castellano
Institut de Chimie Minérale et Analytique, Université de Lausanne
BCH 3307, CH-1015 Lausanne (Switzerland)
Fax: (+41) 21-692-39-05
E-mail: carlo.floriani@icma.unil.ch

[b] Dr. N. Re
Dipartimento di Chimica, Università di Perugia
I-06100 Perugia (Italy)

[c] Prof. Dr. A. Chiesi-Villa, Dr. C. Rizzoli
Dipartimento di Chimica, Università di Parma
I-43100 Parma (Italy)

0947-6539/99/0502-0722 $ 17.50+.50/0 *Chem. Eur. J.* **1999**, *5*, No. 2

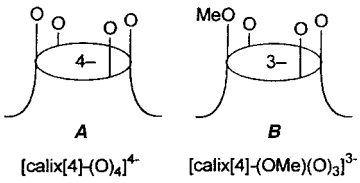

allows the transfer from one model ligand to the other one without affecting the organic functionality bonded to tantalum. We should mention that some of the most relevant results of tantalum organometallic chemistry have been associated with the alkoxo ancillary ligands. This field has been developed, among others, by Rothwell[4] and Wolczanski.[5] Some preliminary results have been communicated.[6]

Results and Discussion

The parent compounds **3** and **4** can be considered a useful entry into the organometallic chemistry of calix[4]arene–tantalum. While the synthesis of **3** from **1** and $TaCl_5$ is straightforward, without the addition of any base, the synthesis of **4** deserves some comments (Scheme 1): the most convenient starting material is **2**, which undergoes demethylation in the reaction with $TaCl_5$ to yield **4**. Demethylation of mono- and dimethoxycalix[4]arene is a simple acid- or base-assisted reaction.[2i] Metals in a high oxidation state induce demethylation with the simultaneous formation of MeCl, via the plausible dimethoxychloro intermediate [*p*-*t*Bu-calix[4]-$(OMe)_2(O)_2TaCl_3$] as in the case of **4**. The demethylation of **4** proceeds further in the presence of a base, such as pyridine, to give **5**, in which the pyridine functions as the acceptor of the methyl carbocation. In both cases, we suppose that the methyl carbocation leaves the calix[4]arene, is captured by a nucleophile from the metal coordination sphere or from the outside. The structure of **3** has been proposed according to that determined for the analogous Nb complex.[7] Accordingly, in the ^{1}H NMR spectrum of **3**, the four *t*Bu groups

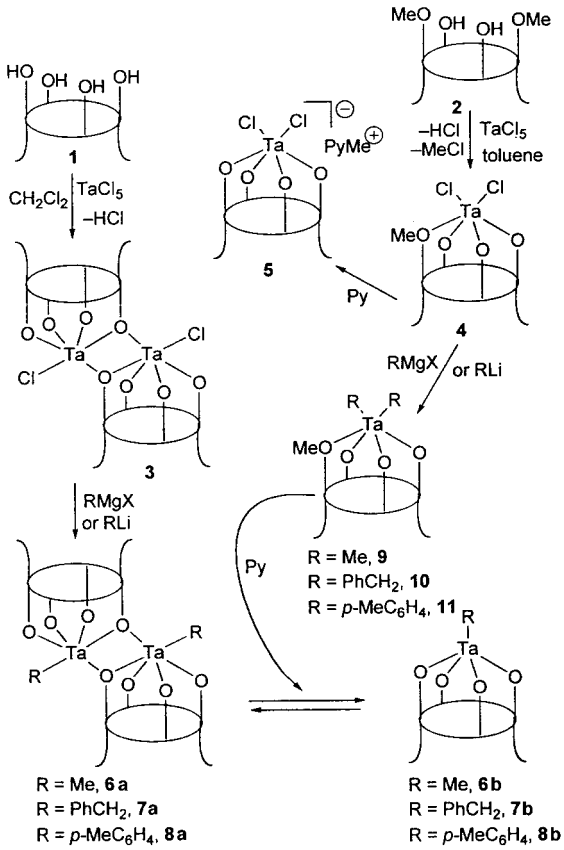

Scheme 1. Synthetic scheme for the parent compounds and their alkylation products.

display three singlets in the ratio 1:1:2, while two pairs of doublets appear for the bridging methylenes. In the spectrum of **5**, a single pair of doublets has been observed along with two singlets for the *t*Bu substituents.

Crystallographic data and details associated with data collection are given in Table 1. Selected bond lengths and angles for complexes **4**, **8a**, **13**, **19**, and **28** are listed in Table 2. Table 3 compares the most relevant conformational parame-

Table 1. Crystallographic data for complexes **4, 8a**, **13**, **19**, and **28**.

	4	**8a**	**13**	**19**	**28**
formula	$C_{45}H_{55}Cl_2O_4Ta \cdot C_7H_8$	$C_{102}H_{118}O_8Ta_2 \cdot 11\,C_5H_5N$	$C_{60}H_{69}O_5Ta \cdot 1.5\,C_6H_6 \cdot 0.5\,C_6H_{14}$	$C_{63}H_{71}NO_4Ta \cdot C_6H_8N \cdot 2.5\,C_6H_6 \cdot C_4H_{10}O$	$C_{102}H_{120}N_2O_8Ta_2 \cdot 4\,C_7H_8$
a [Å]	10.282(2)	17.761(3)	16.399(8)	16.784(3)	14.347(2)
b [Å]	26.422(4)	17.950(3)	17.074(9)	23.934(5)	17.524(3)
c [Å]	18.773(3)	13.029(2)	11.854(5)	19.424(3)	13.088(2)
α [°]	90	109.45(2)	99.10(5)	90	100.57(2)
β [°]	105.10(2)	103.33(2)	107.92(3)	97.00(2)	102.67(2)
γ [°]	90	108.66(2)	88.70(4)	90	108.66(2)
V [Å^3]	4924.0(15)	3436.5(15)	3117(3)	7745(3)	2924.9(10)
Z	4	1	2	4	1
M_r	1003.9	2704.1	1211.4	1450.7	2232.5
space group	$P2_1/c$ (No. 14)	$P\bar{1}$ (No. 2)	$P\bar{1}$ (No. 2)	$P2_1/c$ (No. 14)	$P\bar{1}$ (No. 2)
T [°C]	22	−140	−140	−140	−140
λ [Å]	0.71069	1.54178	0.71069	1.54178	1.54178
ρ_{calcd} [g cm^{-3}]	1.354	1.307	1.291	1.244	1.267
μ [cm^{-1}]	23.55	33.33	17.88	29.85	19.00
transmission coeff.	0.707–1.000	0.812–1.000	0.467–1.000	0.432–1.000	0.383–1.000
R[a]	0.096	0.064	0.061	0.072	0.072
$wR2$[b]	0.288	0.179	0.165	0.223	0.197

[a] $R = \Sigma\,|\,\Delta F\,|\,/\Sigma\,|\,F_o\,|$ calculated on the unique observed data $[I > 2\sigma(I)]$. [b] $wR2 = [\Sigma w\,|\,\Delta F^2\,|^2/\Sigma w\,|\,F_o^2\,|^2]^{1/2}$ calculated on the unique data with $I > 0$.

Table 2. Selected bond lengths [Å] and angles [°] for complexes **4**, **8a**, **13**, **19**, and **28**.

	4	**8a**	**13**	**19**	**28**
Ta(1)–X(1)	2.354(6)	2.106(6)	1.942(4)	1.965(10)	2.042(6)
Ta(1)–X(2)	2.384(6)	2.136(11)	2.100(9)	2.200(15)	2.040(9)
Ta(1)–O(1)	1.802(12)	1.876(6)	1.895(5)	2.017(10)	1.919(8)
Ta(1)–O(2)	2.266(11)	1.912(7)	2.297(6)	1.994(8)	2.320(7)
Ta(1)–O(3)	1.826(9)	2.184(6)	1.900(5)	1.969(9)	1.897(6)
Ta(1)–O(4)	1.867(11)	1.929(7)	1.971(5)	1.995(8)	1.942(6)
O(1)–C(1)	1.387(17)	1.328(11)	1.353(7)	1.323(19)	1.326(13)
O(2)–C(13)	1.42(2)	1.362(13)	1.406(10)	1.398(12)	1.396(13)
O(2)–C(45)	1.47(2)		1.479(9)		1.457(12)
O(3)–C(20)	1.340(18)	1.389(14)	1.349(10)	1.319(17)	1.350(10)
O(4)–C(27)	1.39(2)	1.373(14)	1.375(9)	1.389(14)	1.390(12)
X(1)–X(2)			1.405(11)	1.43(2)	
O(3)-Ta(1)-O(4)	90.6(5)	84.4(2)	90.0(2)	82.6(3)	90.0(3)
O(2)-Ta(1)-O(4)	164.6(4)	154.1(3)	157.9(3)	157.7(3)	158.6(3)
O(2)-Ta(1)-O(3)	79.0(4)	84.9(3)	81.1(2)	81.7(3)	76.7(3)
O(1)-Ta(1)-O(4)	89.0(4)	83.9(3)	91.0(2)	87.0(4)	88.7(3)
O(1)-Ta(1)-O(3)	94.6(5)	126.6(3)	136.0(3)	126.5(3)	101.4(3)
O(1)-Ta(1)-O(2)	80.6(4)	83.6(3)	81.8(2)	89.8(4)	77.9(3)
X(1)-Ta(1)-X(2)	85.0(2)	80.4(4)	40.4(3)	39.7(5)	75.6(3)
Ta(1)-O(1)-C(1)	152.4(10)	161.9(7)	152.4(5)	131.0(9)	169.3(6)
Ta(1)-O(2)-C(45)	129.5(12)		128.8(5)		128.1(6)
Ta(1)-O(2)-C(13)	117.3(9)	136.9(6)	118.6(4)	126.6(7)	118.2(5)
C(13)-O(2)-C(45)	113.2(13)		112.6(6)		113.7(8)
Ta(1)-O(3)-C(20)	169.9(10)	113.8(6)	154.9(5)	164.8(8)	169.3(7)
Ta(1)-O(4)-C(27)	125.5(10)	134.5(6)	122.9(5)	124.1(6)	121.8(6)
Ta(1)-X(1)-Ta(1)′		114.6(3)			104.4(3)
Ta(1)-X(1)-X(2)			75.8(4)	79.1(7)	
Ta(1)-X(2)-X(1)			63.7(4)	61.3(6)	
Ta(1)′-X(1)-C(51)					128.0(6)
Ta(1)-X(1)-C(51)					127.5(6)

[a] X(1) = Cl(1), O(4)′, O(5), and N(1) for **4**, **8a**, **13**, **19**, and **28**, respectively; X(2) = Cl(2), C(51), C(51), and N(1)′ for **4**, **8a**, **13**, **19**, and **28**, respectively. A prime denotes a transformation of $-x, -y, -z$ and $-x, 1-y, -z$ for **8a** and **28**, respectively.

Table 3. Comparison of the relevant conformational parameters within calixarene for complexes **4**, **8a**, **13**, **19**, and **28**.

	4	**8a**	**13**	**19**	**28**
Dihedral angles [°] between planar moieties[a]					
∢E–ring A	157.6(4)	156.0(3)	132.1(2)	123.3(3)	148.1(2)
∢E–ring B	110.5(4)	127.9(3)	110.4(2)	115.5(3)	107.7(2)
∢E–ring C	147.1(4)	107.6(3)	134.1(2)	152.9(3)	146.7(3)
∢E–ring D	118.2(4)	128.0(3)	115.5(2)	112.9(3)	112.6(2)
∢ring A–ring C	124.7(5)	106.3(4)	95.8(2)	95.5(4)	114.8(3)
∢ring B–ring D	131.3(5)	103.8(3)	134.0(2)	131.4(4)	139.7(3)
Contact distances [Å] between *para*-carbon atoms of opposite aromatic rings					
C4···C17	10.01(3)	8.234(14)	9.182(12)	8.38(2)	9.956(14)
C10···C24	7.46(3)	8.727(18)	7.306(13)	7.372(18)	7.046(13)

[a] E = Reference plane and refers to the least-squares mean plane defined by the bridging methylenic carbons C(7), C(14), C(21), and C(28).

ters for the four complexes. The aromatic rings of the phenolic units containing O(1), O(2), O(3), and O(4) are referred to as A, B, C, and D, respectively. The structure of **4** is depicted in Figure 1.

The macrocycle has an elliptical cross-section with the opposite-facing A and C rings pushed outwards and the B and D rings pulled into the cavity, as indicated by the dihedral angles they form with the reference plane (Table 3) and by the values of the distances between opposite *p*-carbon atoms

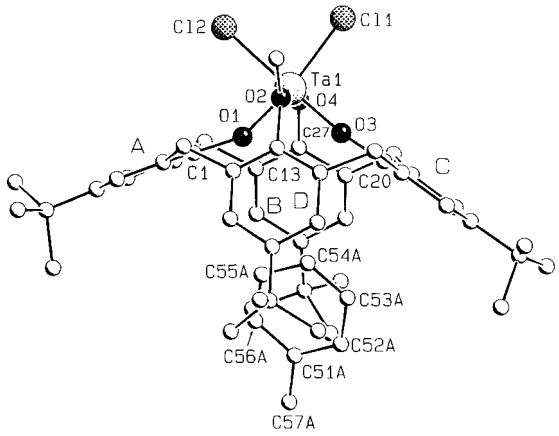

Figure 1. A SCHAKAL view of complex **4**. Disorder has been omitted for clarity.

[C(4)···C(17), 10.01(3) Å; C(10)···C(24), 7.46(3) Å]. The guest toluene molecule was found to be statistically distributed over two positions (A and B). In both positions the molecule is oriented with the methyl group pointing outside the cavity. The octahedral coordination around tantalum involves the four oxygen atoms from the methoxycalixarene ligand and two *cis*-arranged chlorine atoms. The best equatorial plane is defined by the O(1), O(3), Cl(1), Cl(2) donor atoms [maximum deviation from planarity is 0.021(11) Å for O(3)]; the metal lies out of this plane by 0.183(1) Å towards O(4). The hexacoordination of the metal removes the planarity of the O_4 core, which shows remarkable tetrahedral distortions that range from −0.503(11) to 0.535(12) Å. The values of the Ta–O bond lengths with O(1), O(3), and O(4) [mean value 1.832(18) Å] fall in a narrow range and are noticeably shorter than the Ta–O(2) bond length [2.266(11) Å] from the methoxy group. The bond angles Ta-O(1)-C(1) [152.4(10)°] and Ta-O(3)-C(20) [169.9(10)°], which are considerably larger than the bond angles Ta-O(2)-C(13) [129.5(12)°] and Ta-O(4)-C(27) [125.5(10)°], are consistent with a Ta–O π interaction.

The alkylation of **3** furnished the corresponding alkyl/aryl derivatives (Scheme 1), which have been obtained as light yellow, thermally stable, crystalline solids. Although the solid-state structures of **7** and **8** (vide infra) reveal their dimeric nature, solutions of compounds **6–8** are in equilibrium with their corresponding monomeric form. As can be judged from the ^{1}H NMR spectrum, such an equilibrium is completely shifted to the right in the case of **7**, while in the case of **6** and **8** both forms are equally present in solution. The X-ray structure of **7a** is reported in the material deposited with the Cambridge Crystallographic Data Centre (see Experimental Section). The structure of **8a** consists of centrosymmetric dimers (Figure 2). The O_4 core shows remarkable tetrahedral distortions (displacements from planarity), which range from −0.260(8) to 0.238(8) Å, while tantalum lies 0.667(2) Å out of the mean plane. The planar Ta_2O_2 ring is perpendicular to the O_4 core; the dihedral angle they form is 88.5(7)°. The Ta···Ta′ separation is 3.609(2) Å. The Ta–O(1) bond length [1.876(6) Å] is significantly shorter than those of Ta–O(2) and Ta–O(4) [mean value 1.921(9) Å], in accor-

0947-6539/99/0502-0724 $ 17.50+.50/0 *Chem. Eur. J.* **1999**, *5*, No. 2

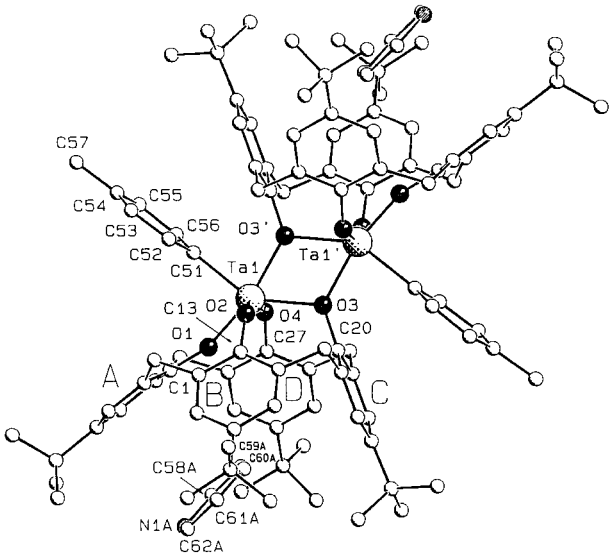

Figure 2. A SCHAKAL view of complex **8a**. The prime denotes a transformation of $-x, -y, -z$. Disorder has been omitted for clarity.

dance with the Ta-O(1)-C(1) bond angle [161.9(7)°]. Rather long bond lengths are found for the bridging oxygen O(3) [Ta–O(3), 2.184(6) Å; Ta–O(3)′, 2.106(6) Å]. The Ta–C(51) bond length [2.136(11) Å] falls in the lower range of values reported for Ta–C(primary alkyl) σ bonds [mean value 2.204(14) Å].[4, 5] The conformation of the calixarene macrocycle has an asymmetrical elliptical cross-section (Table 3).

Reaction of **4** with Grignard reagents led to **9**–**11**, which are all equally thermally stable in boiling benzene for 24 h. However, depending on the R substituent, they display different reactivities under various conditions. All of them undergo demethylation to **6**–**8** in the presence of pyridine. The byproducts of the reaction are the R–R coupled hydrocarbons and a mixture of alkylated pyridines. For comments on the demethylation mechanism see below. The benzyl derivative **10** undergoes demethylation quite readily in the presence of light or under an atmosphere of H_2.

The migratory insertion reactions of the Ta–C functionalities in complexes **9**–**11** are presented in Scheme 2.[8] In the reaction of **9**–**11** with either CO or *t*BuNC, we observed the migration, under mild conditions (i.e. room temperature), of both alkyl and aryl groups to afford η^2-ketones **12**–**14** and η^2-imino derivatives, **15**–**17**. Unlike the case of $[Cp_2M]$ or polyphenoxo derivatives of Ta, migration of the second alkyl or aryl group to produce the intermediate η^2-acyl or η^2-iminoacyl derivatives is very fast, which prevented us from intercepting the precursor.[8, 9] As with the $[(\eta^8\text{-}C_8H_8)ZrR_2]$ derivatives,[10] such a pathway is assisted by the presence on the metal of the three facial frontier orbitals (vide infra). All the η^2-ketone and η^2-imino compounds have been fully characterized by ^{1}H NMR spectroscopy in solution and their structure is exemplified by that of **13**, shown as a SCHAKAL representation in Figure 3. Coordination around tantalum is determined by the four oxygen atoms from calixarene and by the O(5) and C(51) atoms from dibenzylketone. The Ta–O(5) and Ta–C(51) bond lengths are consistent with an asymmetric η^2-C,O-interaction [Ta–O(5), 1.942(4) Å; Ta–C(51),

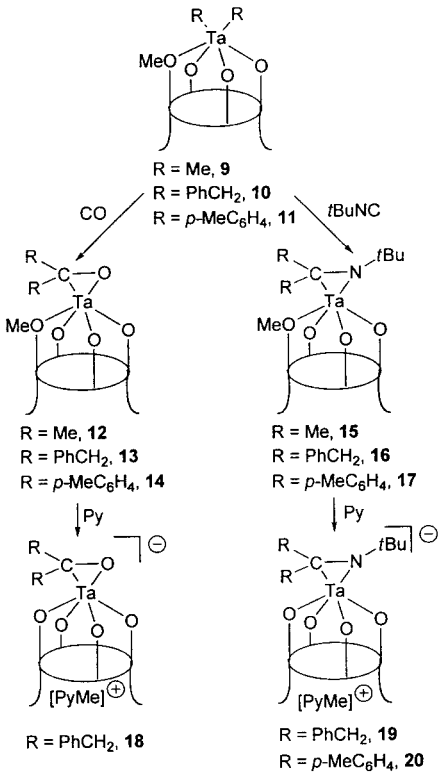

Scheme 2. Migratory insertion reactions into the Ta–C bonds.

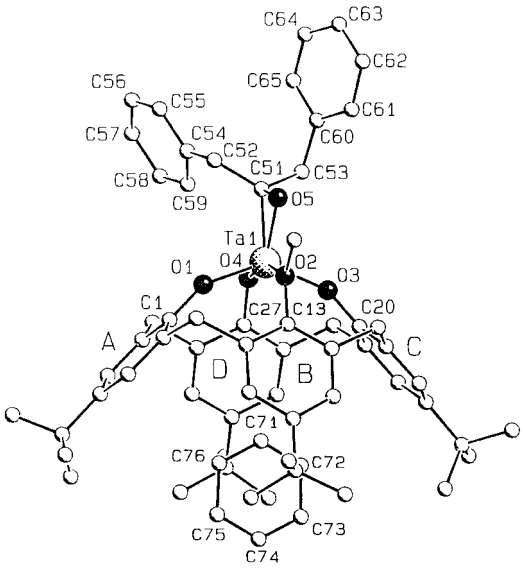

Figure 3. A SCHAKAL view of complex **13**. Disorder has been omitted for clarity.

2.100(9) Å]. The two-electron reduced form of the ketone is supported by the O(5)–C(51) bond length [O(5)–C(46), 1.405(11) Å]. The O_4 core shows tetrahedral distortions which range from −0.144(6) to 0.144(6) Å and the metal atom is displaced by 0.550(3) Å out of the mean plane towards the η^2-C,O-bonded ligand. The plane through the η^2-bonded atoms [Ta, O(5), C(51)] is perpendicular to the O_4 core; the dihedral angle they form is 90.6(3)]°. The Ta–O bond lengths and related Ta-O-C angles (Table 2) suggest a significant π interaction of the metal, essentially with O(1) and O(3), and

none with the methoxy group O(2). As a consequence, the conformation of the calixarene cavity assumes an elliptical cross-section, as indicated by the values of the distance between opposite *p*-carbon atoms: C(4)···C(17) 9.182(12) Å; C(10)···C(24) 7.306(13) Å (Table 3).[11]

Both classes of compounds **12**–**14** and **15**–**17** are particularly thermally stable and the M–C bond does not undergo a further insertion reaction. They can be quite sensitive to the presence of a base which causes demethylation and formation of the corresponding anionic species, as illustrated by the reaction of **13**, **16**, and **17** with pyridine. This reaction, which leads to **18**–**20**, has been followed by NMR; however, only products **19** and **20** were isolated. Although the reaction of **4**, **9**–**11**, **13**, **16**, and **17** with bases, and particularly with pyridine, led to the demethylation of the monomethoxycalix[4]arene independently of the functional group attached to the metal, this group does affect the reaction pathway: in the case of the chloride (complex **4**), η^2-ketones (complexes **12**–**14**), or η^2-imines (complexes **15**–**17**), the π-donating ability of the functional groups makes the metal less accessible to outside attack. Thus the pyridine will remove the methyl carbocation from the methoxy group without the assistance of the metal and forms, almost exclusively, a pyridine-methyl cation. In the case of the dialkyl derivatives **9**–**11**, where the metal is more electrophilic (vide infra), the assistance of the metal is much more likely and led, through a much more complex mechanism, to a mixture of by-products, such as the alkylated forms of pyridine and the coupled alkyl residues. It should be emphasized that it is unlikely that the formation of **18**–**20** can be achieved by another synthetic route.

The nature of an anionic form of the η^2-metal bonded ketone or imine is exemplified by the structure of **19** (Figure 4): the pyridinium cation is hosted inside the calix[4]-arene cavity. Coordination around tantalum is provided by the four oxygen atoms from calixarene and by the N(1) and C(51) atoms from the imino ligand. The Ta–N(1) and Ta–C(51) bond lengths are consistent with a slightly asymmetric η^2-N,C-interaction [Ta–N(1) 1.965(10) Å; Ta–C(51), 2.200(15) Å], while the N(1)–C(51) bond length [1.43(2) Å] is that of a single bond. The O_4 core shows remarkable tetrahedral distortions which range from −0.284(9) to 0.254(8) Å, and the metal is displaced by 0.618(1) Å out of the mean plane towards the η^2-N,C-bonded ligand. The plane through the η^2-bonded atoms [Ta, N(1), C(51)] is almost perpendicular to the O_4 core; the dihedral angle they form is 93.0(4)]°. The Ta–O bond lengths, which are not remarkably different (Table 2), and the Ta-O-C angles are in agreement with a Ta–O π interaction. The bond lengths of Ta–N(1) [1.965(10) Å] and Ta–C(51) [2.200(15) Å] are close to the values reported in the literature [mean values 1.955(9) and 2.209(25) Å for Ta–N and Ta–C bond lengths, respectively].[12] The conformation of the calixarene macrocycle assumes an elliptical cross-section, as indicated by the values of the distance between opposite *p*-carbon atoms: C(4)···C(17) 8.38(2) Å; C(10)···C(24) 7.372(18) Å (Table 3). The methylpyridinium cation sits in the cavity of the calixarene and the aromatic ring is oriented nearly perpendicularly to the A and C rings [dihedral angles 86.4(4) and 89.9(4)°, respectively] and parallel to the B and D rings [dihedral angles 26.1(3) and 23.3(3)°, respectively.

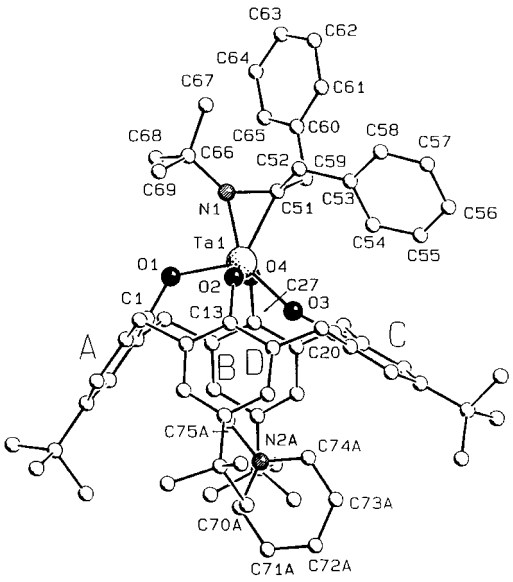

Figure 4. A SCHAKAL view of complex **19**. Disorder has been omitted for clarity.

It has to be mentioned that, under the same conditions, the alkyl and aryl derivatives **6**–**8** do not undergo any migratory insertion reaction with CO, RNC, or olefins. This is not surprising because complexes **6b**–**8b**, though in a monomeric form, do not bind pyridine, which would simulate the precoordination of a substrate preceding a migratory insertion reaction with carbon monoxide and isocyanide. In the latter case, the only detectable reaction was the reversible formation of an adduct when **7** was reacted with *t*BuNC. The reaction was followed both by IR and NMR spectroscopy (see Experimental Section) at different temperatures. The proton chemical shift of the *t*Bu [*t*BuNC], in particular, clearly indicates a coordination of isocyanide within the calix[4]arene cavity.

Complex **4** can also be used as a starting material to synthesize complexes which contain unsaturated carbon functionalities that are bonded to the metal (Scheme 3). Very probably, the reaction with LiC≡CPh proceeds through the formation of a bis(phenylacetylide) derivative **A** (Scheme 3), which then reacts with a third equivalent of LiC≡CPh by an attack of the α-carbon of one of the acetylide ligands to form **21**. Complex **21** contains a σ-bonded acetylide, and an η^2-bonded 1,4-diphenylbutadiyne, Ph–C≡C–C≡C–Ph. The addition of yet a further equivalent of LiC≡CPh is, very probably, prevented by the existence of only three available frontier orbitals on the [calix[4]-$(OMe)(O)_3$Ta] fragment; the fourth orbital is only available for nonbonding electrons (vide infra). The low-quality X-ray structure of **21** is reported in the material deposited with the Cambridge Crystallographic Data Centre (see Experimental Section). Reaction of **4** with allyl-MgCl led to the complete replacement of both chlorides and to the formation of the bis(allyl) derivative **22**, which has been isolated as a yellow microcrystalline solid. The η^3-bonding mode of both allyl groups (shown in Scheme 3) is supported by the ^{1}H NMR spectrum (see the Experimental Section), which did not change as a function of the temperature. Complex **22** behaves in a similar manner to σ-bonded alkyl or

0947-6539/99/0502-0726 $ 17.50+.50/0 *Chem. Eur. J.* **1999**, *5*, No. 2

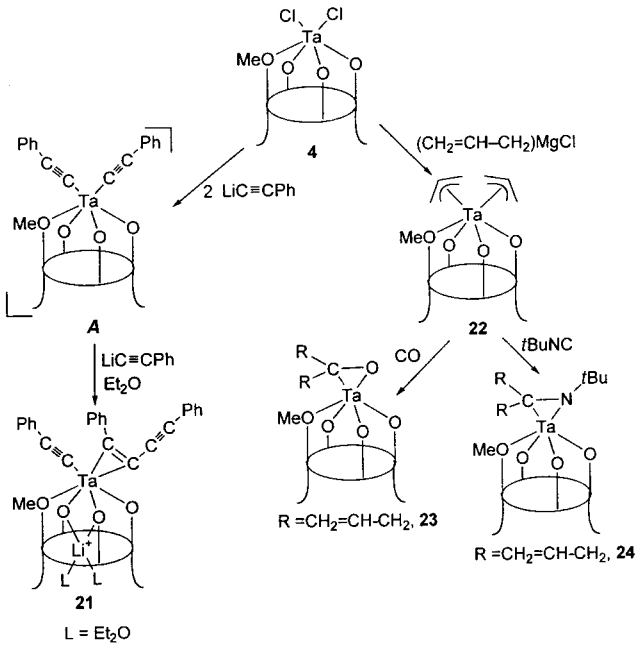

Scheme 3. Synthesis and reactivity of allyl and acetylide derivatives of Ta–monomethoxycalix[4]arene.

aryl derivatives undergoing migratory insertion with CO and *t*BuNC to give **23** and **24**, respectively. They apparently do not display any particularities as compared with the analogous derivatives **12**–**17**, and have been fully characterized (see the Experimental Section).

The tantalum–butadiene derivative **25** was obtained from the reaction of **4** with $[Mg(C_4H_6)]$ in the form of an orange microcrystalline solid (Scheme 4). The tantalum–butadiene

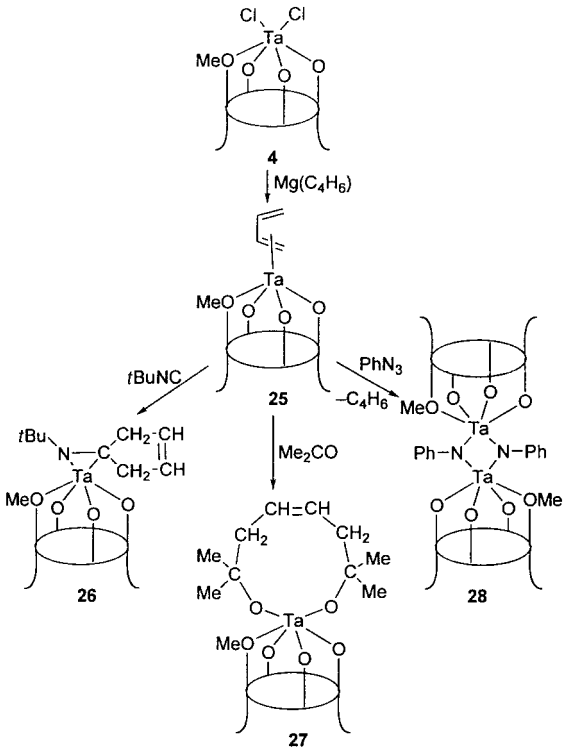

Scheme 4. Synthesis and reactivity of Ta–butadiene bonded to monomethoxycalix[4]arene.

functionality exists in various forms in the cyclopentadienyl series,[13] while **25** is a quite unusual compound in tantalum–alkoxo organometallic chemistry. The *cis*-π^2,η^4-bonding mode we suggest for **25** is unlike that found in many of the cyclopentadienyl derivatives,[13] and is essentially based on the information from NMR and theoretical studies (vide infra). The chemistry and structural features of **25** parallel those of the analogous $[p$-*t*Bu-calix[4]-$(OMe)_2(O)_2Zr(\eta^4$-$C_4H_6)]$.[14] Three different modes of reaction have been identified towards *t*BuNC, PhN_3, and Me_2CO. In the reaction with *t*BuNC, the butadiene ligand behaves as though it is bonded to the metal in a η^4,σ^2-π fashion and affords the imino complex **26**, as a consequence of a double migration such as we observed for the complexes **9**–**11**. Butadiene behaves in a similar manner in the reaction with acetone, to give the nine-membered dioxo metallacycle, **27**. In the reaction with PhN_3, complex **25** behaves as a source of the d^2-tantalum(III) fragment $[p$-*t*Bu-calix[4]-$(OMe)(O)_3Ta]$ to give a phenylimido derivative (Scheme 4), that is the μ-phenylnitrene dimer **28**. In addition to the analytical and spectroscopic data, the structures of **27** (very preliminary) and **28** received further support from their X-ray analysis.

The structure of **28** consists of centrosymmetric dimers (Figure 5). The conformation of the macrocycle assumes an elliptical cross-section similar to that observed in **4** (Table 3). This conformation enables a toluene solvent molecule to be

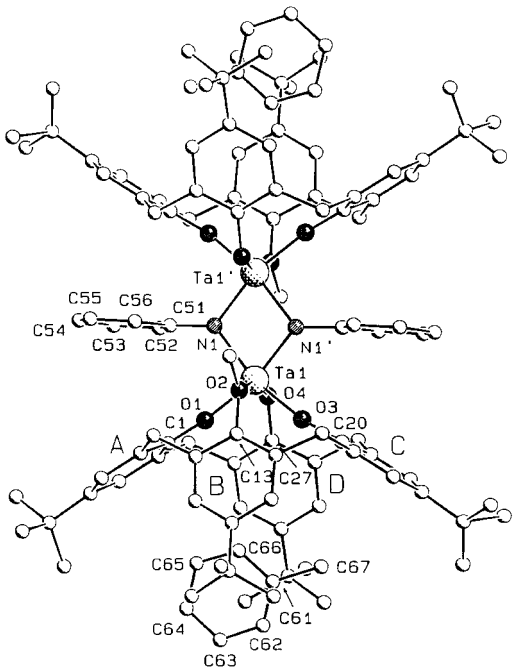

Figure 5. A SCHAKAL view of complex **28**. The prime denotes a transformation of $1-x$, $1-y$, $1-z$. Disorder has been omitted for clarity.

accommodated inside the cavity as a guest with the aromatic ring oriented nearly perpendicular to the A and C rings [dihedral angles 87.2(4) and 87.3(3)°, respectively] and parallel to the B and D rings [21.1(3) and 19.2(3)°, respectively].[15] The metal exhibits a distorted octahedral coordination; the O(1), O(3), N(1), N(1)′ atoms define the best equatorial plane

out of which tantalum is displaced by 0.166(1) Å towards O(4). As observed in complex **4**, the hexacoordination of the metal removes the planarity of the O_4 core, which shows remarkable tetrahedral distortions, which range from −0.421(7) to 0.417(7) Å, while tantalum is displaced by 0.771(1) Å out of the mean plane. The Ta_2N_2 ring, which is planar from symmetry requirements, is perpendicular to the O_4 core; the dihedral angle between the two planes is 88.0(2)°. The Ta···Ta′ separation is 3.226(1) Å. The C(51)···C(56) aromatic ring is nearly perpendicular to the Ta_2N_2 core; the dihedral angle is 84.63°. The Ta–O and Ta-O-C parameters (Table 2) support a significant π interaction between the metal and O(1) and O(3). The Ta–N bond lengths [mean value 2.041(1) Å] are in good agreement with the values reported for complexes containing bridging imido groups [mean value 2.029(4) Å calculated with 8 complexes].[16]

Extended Hückel analysis: Extended Hückel calculations[17] were performed to gain a better understanding of the main electronic and structural properties of the tantalum complexes supported by the calix[4]arene-O_4 matrix and their reactivity patterns. The aim of these calculations is: i) to study the frontier orbitals of the organometallic building blocks, in which the tantalum is anchored, to mono- and unmethylated calix[4]arene matrices and their consequences on the reactivity of these organometallic fragments, ii) to study the base-assisted demethylation of **4** and **9**, iii) to study the migratory insertion of CO in **6** and **9**, and iv) to provide insight into the nature of the bonding between tantalum and butadiene in **25**.

Two organometallic fragments have been considered in which the tantalum is coordinated by the nonmethylated and monomethylated forms of calix[4]arene, that is [calix[4]-$(O)_4$Ta]$^+$ and [calix[4]-(OMe)$(O)_3$Ta]$^{2+}$, respectively. The ligands have been slightly simplified by replacing the *t*Bu groups and the methylene bridges by hydrogens, and by applying C_{4v} and C_s symmetries, respectively. This simplified model retains the main features of the whole ligand; in particular the geometrical constraints on the O_4 set of donor atoms has been maintained by fixing the geometry of the four phenoxo groups to the experimental values observed for the mono- or dichloro derivatives.

The lowest unoccupied orbitals of these fragments are depicted in Figure 6. For both these Ta^V species with a d^0 electron count, we found four low-lying, empty, metal-based orbitals. The $d_{x^2-y^2}$, which point more closely towards the oxygen ligands, are pushed higher in energy while the remaining four d orbitals are found within 1 eV of each other. For the [calix[4]-$(O)_4$Ta] fragment the LUMO is a $1a_1(d_{z^2})$ with a doubly degenerate $1e(d_{xz}, d_{yz})$ about 0.5 eV above it. Due to in-plane π interactions with the four oxygen atoms, the $1b_2(d_{xy})$ orbital is destabilized and lies 0.5 eV higher in energy.

In the [calix[4]-(OMe)$(O)_3$Ta]$^+$ fragment, due to the reduced σ and π interactions with the methylated phenoxo ligand in the xz plane, the (d_{xz}, d_{yz}) set is expected to split; the d_{xz} component would be lower in energy and closer to the (d_{z^2}). Moreover, because of the lower molecular symmetry (C_s), the two lowest orbitals of d_{z^2} and d_{xz} character have the same a′ symmetry and mix strongly to give rise to two

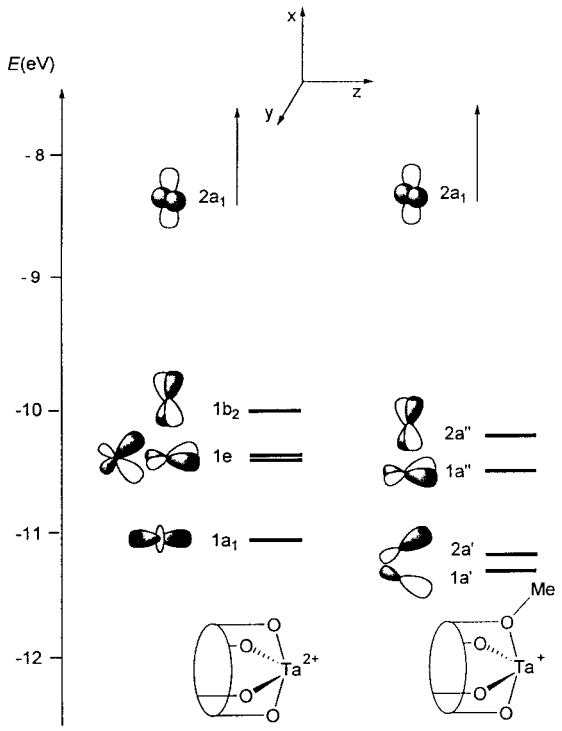

Figure 6. Lowest unoccupied orbitals of the [calix[4]-$(O)_4$Ta]$^+$ and [calix[4]-(OMe)-$(O)_3$Ta]$^{2+}$ fragments.

hybridized 1a′ and 2a′ orbitals lying in the xz plane and tilted, respectively, towards the (O) and (O–Me) directions (see also Figure 7).

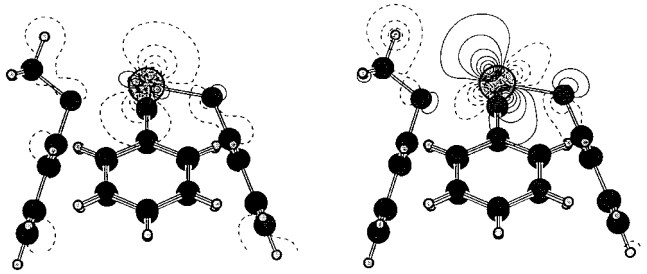

Figure 7. The lowest 1a′ and 2a′ orbitals of the [calix[4]-(OMe)$(O)_3$Ta]$^{2+}$ fragment.

Most of the structures discussed in this work can be easily rationalized on the basis of the frontier orbitals of the above fragments. Let us first consider the hexacoordinated compounds formed by the monomethylated calixarene fragment with two mainly σ-bonding ligands, that is [calix[4]-(OMe)$(O)_3$Ta X_2] [X = Cl (**4**), Me (**9**)], in which the two X^- ligands lie in the Ta$(O)_2$ plane (yz). Only two of the low-lying d orbitals are used, notably the d_{z^2} and d_{yz}, which interact with the in-phase and out-of-phase combinations, respectively, of the two σ orbitals of the X^- groups, to leave as the LUMO an a′ orbital of essentially d_{xz} character with the a″(d_{xy}) orbital slightly higher in energy. A difference is, however, observed between the dialkyl and dichloro compounds: for a purely σ-donating ligand, such as Me, the metal orbitals of the [calix[4]-(OMe)$(O)_3$Ta]$^{2+}$ fragment not involved in the M–X bonding,

0947-6539/99/0502-0728 $ 17.50+.50/0 *Chem. Eur. J.* **1999**, *5*, No. 2

a′ (d_{xz}) and a′ (d_{xy}), remain essentially unaltered at about the same energies observed for the [calix[4]-$(OMe)(O)_3Ta]^+$ fragment. A different situation is found when we consider a π-donor ligand, such as Cl^-, where the interaction with the π-donor orbitals of Cl^- results in a destabilization of these two metal orbitals which are therefore considerably higher in energy. This difference between the two complexes has important consequences on their base-assisted demethylation (vide infra).

We then considered the behavior of the [calix[4]$(O)_4TaX$] compounds [X = Cl (**3**), Me (**6b**)] and assumed an idealized monomeric pentacoordinated structure in which the X^- ligand lies along the z axis. In these species we have a strong bonding interaction between the metal d_{z^2} and the σ orbital of X^-. For a purely σ-donating ligand, such as Me, the remaining low-lying orbitals of the metal fragment remain essentially unaltered so that the LUMO is the 1e (d_{xz}, d_{yz}) pair, while for a π-donor ligand, such as Cl^-, the interaction with the π-donor orbitals leads to a destabilization of the 1e (d_{xz}, d_{yz}) to leave the $1b_2$ (d_{xy}) as a singly occupied orbital.

We now turn our attention to the base-induced demethylation of **4** and **9** which leads to [calix[4]-$(O)_4TaCl_2]^-[PyMe]^+$ (**5**), and [calix[4]-$(O)_4$TaMe] (**6b**), respectively. This reaction was modeled with the help of a NH_3 molecule. An analysis of the frontier orbitals and of the Mulliken charges of **4** and **9** shows that in both cases the LUMO orbitals are essentially localized on the tantalum and that it also bears the highest positive charge. Therefore, we expect the metal to be the most electrophilic center in these compounds and to undergo direct attack by the base. The spatial extension of the a′ (d_{xz}) LUMO suggests that the favorable approach of the nucleophilic NH_3 species occurs along a line in the xz plane which forms an angle of approximately 45° with the z-axis. We first simulated the initial stages of the NH_3 attack by performing extended Hückel calculations on the [calix[4]-$(OMe)(O)_3TaX_2$]-NH_3 system (X = Cl, Me) with different (NH_3)-to-metal distances (L), (5.0 to 2.5 Å), along the expected most favorable line. At each point along the attack pathway we relaxed the X-Ta-X angle, the dihedral angle between the $TaMe_2$ and $Ta(O)_2$ planes, and the angular position of NH_3. The two total energy profiles (Figure 8) show that the attack on the metal is far more energetically favorable for the bis(methyl) than for the bis(chloro) complex. For the bis(methyl) complex a small activation barrier is observed at ≈3 Å, although this is not followed by a significant stabilization at shorter distances. Instead, in the case of the bis(chloro) complex, the energy profile reaches 2 eV at the shortest considered distance of 2.5 Å. This implies that the bis(chloro) complex is less electrophilic than the bis(methyl) analogue, which is in agreement with the higher energy of the LUMO orbital (−9.7 versus −10.6 eV) and the lower charge on tantalum (+1.0 versus +1.1). The analysis reported in Figure 8 suggests that demethylation is probably a metal-assisted process in the case of **9**–**11**, while we can admit a direct attack of the base on the positively charged methyl (+0.34) in the case of complex **4**.

The complexes reported here are appropriate models to study the migratory insertion reaction of CO into a M–C bond anchored to an oxo surface. We started this study by examining the reaction of carbon monoxide with **9**. We first simulated the initial stages of the attack of CO by performing extended Hückel calculations on the [(calix[4]-$(OMe)(O)_3$-$TaMe_2$]-CO system with different (CO)-to-metal distances (5.0 to 2.5 Å) along the expected most favorable line (see above). At each point along the attack pathway we relaxed the Me-Ta-Me angle, the dihedral angle between the $TaMe_2$ and $Ta(O)_2$ planes, and the angular position of CO. The total energy profile (Figure 8) shows an energy barrier of only 0.5 eV followed by a significant stabilization, which thus allows the facile insertion of CO into the Ta–C bond to give an η^2-acyl intermediate. We have considered this hypothetical intermediate [calix[4]-$(OMe)(O)_3$TaMe(η^2-COMe)] in the idealized structure ***C*** (Scheme 5) with the planar η^2-acyl moiety lying perpendicular to the $TaMe_2$ reference plane of

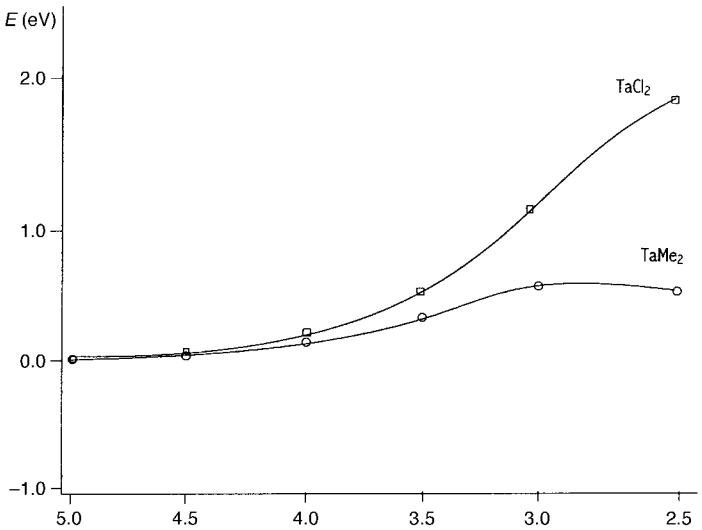

Figure 8. Total energy profile for the attack of NH_3 on tantalum in [calix[4]-$(OMe)(O)_3TaX_2$].

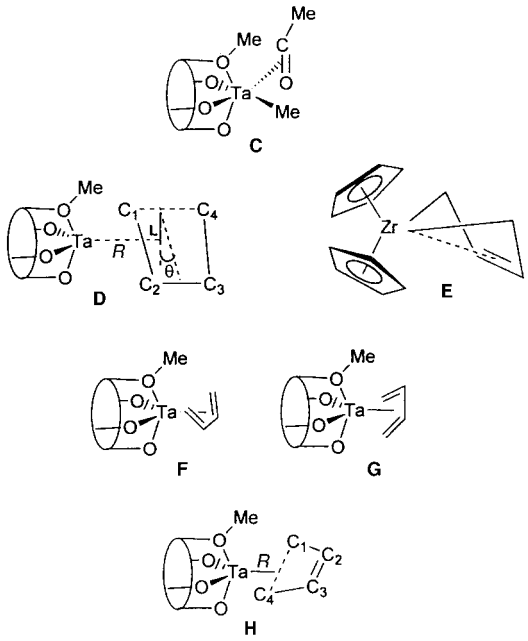

Scheme 5. η^2-Acyl (**C**) and butadiene (**D, F, G, H**) bonding modes to Ta–calix[4]arene moieties and to Cp_2Zr (**E**).

the dimethyl reagent (*yz* in our frame). Previous calculations[2e] on the analogous intermediate compound [calix[4]-$(OMe)_2(O)_2$ZrMe(η^2-COMe)] have shown that this is the most stable structure, at variance with the structurally characterized zirconium bis(cyclopentadienyl)-methyl η^2-acyl species [Cp_2ZrMe(η^2-COMe)] in which the planar η^2-acyl moiety lies in the $ZrMe_2$ reference plane of the dimethyl reagent. This structural difference has already been discussed and interpreted in terms of the different nature of the low-lying metal orbitals for the $[Cp_2Zr]^{2+}$ and [calix[4]-$(OMe)_2(O)_2Zr]^{2+}$ fragments. For the $[Cp_2Zr]^{2+}$ fragment only orbitals in the equatorial plane are available; this permits only meridional geometries and rules out nonplanar structures, such as ***C***, while for [calix[4]-$(OMe)_2(O)_2Zr]^{2+}$ as well as for [calix[4]-$(OMe)(O)_3Ta]^{2+}$ there are vacant low-energy orbitals lying on both the perpendicular symmetry planes.

An analysis of the orbital energies and the charge on the acyl and methyl carbon atoms in [calix[4]-$(OMe)(O)_3$Ta Me(η^2-COMe)] helps to explain the fast migration of the second alkyl in the hypothetical species [calix[4]-$(OMe)(O)_3$-TaMe(η^2-COMe)], which leads to the η^2-ketone complex. Hoffmann et al. have shown that the reactivity of such an η^2-coordinated acyl can be described in terms of its *carbenium-type* character, and is determined by a positive charge on the carbon atom and the presence of a low-lying LUMO, made up essentially of the π^*_{CO} perpendicular to the acyl plane.[18] Both effects make the acyl carbon electrophilic; this favors its insertion into the second alkyl group to give the η^2-ketone. Our calculations on [calix[4]-$(OMe)(O)_3$Ta Me(η^2-COMe)] showed a significant charge on the acyl carbon (+0.5) and a low-energy π^*_{CO} orbital (−9.9 eV), which suggests a facile attack by the second alkyl group of carbanion character (the methyl carbon bears a negative charge of −0.3) with the formation of the η^2-ketone. This insertion of CO into metal–calix[4]arene dialkyl complexes, which leads directly to a η^2-ketone without the formation of an intermediate η^2-acyl species, has already been observed for analogous [calix[4]-$(OMe)_2(O)_2ZrR_2$] compounds. It is at variance with the behavior of bis(cyclopentadienyl)dialkyl complexes of early transition metals, for which the η^2-acyl intermediate has been isolated and structurally characterized (see ref. [2e] for a discussion of this difference in behavior). In the case of the monoalkyl derivatives **6**–**8**, for which no migratory insertion of CO or *t*BuNC has been observed, the energy profile for the approach of CO towards the metal (Figure 9) looks quite different and shows strong stabilization upon the coordination of CO to tantalum. Such a profile was obtained by adjusting only the angular position of CO and methyl. This result would suggest the formation of a stable CO adduct which does not undergo any migratory insertion. As a matter of fact, in the reaction of **7** with *t*BuNC (see preceding section), a reversible coordination of *t*BuNC was found. The lack of a migration reaction may be due either to the thermodynamically unfavorable formation of an η^2-acyl or η^2-iminoacyl intermediate, which, in the present case, cannot evolve to the stable η^2-ketone or η^2-imine, or even to the binding of CO and RNC to the metal, but rather to the coordination of *t*BuNC inside the cavity of the calix[4]arene. Such a geometrical alkyl–CO reciprocal arrangement would prevent any migratory insertion reaction. Significant support for the coordination of RNC inside the cavity comes from the reaction of *t*BuNC with **7**, where such a kind of binding was observed.

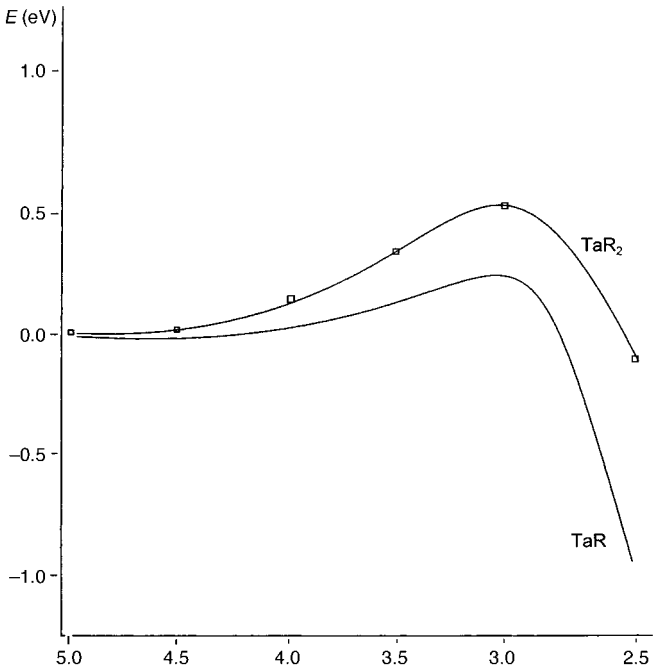

Figure 9. Total energy profile for the attack of CO on tantalum in [calix[4]-$(OMe)(O)_3TaMe_2$] and in [calix[4]-$(O)_4$TaMe].

Extended Hückel calculations were also performed to elucidate the nature of the bonding between the butadiene unit and the central metal in complex **25**. The coordination geometry of the butadiene unit was optimized with respect to the three parameters *R*, *L*, and θ depicted in Scheme 5 (***D***), while all the other geometrical parameters were kept fixed. *R* represents the distance of the butadiene from tantalum, *L* defines its departure from the main symmetry axis (z) of the metal fragment, while θ represents the dihedral angle between the butadiene plane and the reference plane of the fragment. The geometrical parameters taken for the metal fragment were Ta–O = 1.99 (phenoxy), Ta–O = 2.35 (Me-phenoxy), O–C(Ph) = 1.33 (phenoxy), O–C(Ph) = 1.41 (Me-phenoxy), O–C(Me) = 1.43, O-Ta-O = 114° (phenoxy), O-Ta-O = 153° (Me-phenoxy), Ta-O-C(Ph) = 172° (phenoxy), Ta-O-C(Ph) = 116° (Me-phenoxy), and Ta-O-C(Me) = 131°. The butadiene moiety was considered as a planar unit with the geometrical parameters taken from the analogous [calix[4]-$(OMe)_2(O)_2$Zr(butadiene)] complex:[14] $C_1–C_2 = 1.43$, $C_2–C_3 = 1.44$, C–H = 1.09, C_1-C_2-C_3 = 120°, and C-C-H = 120°. The minimum was calculated for *R* = 1.95 Å, *L* = 0.75 Å, and θ = 15°, which corresponds to a π^2,η^4 structure, in agreement with the ^{1}H and ^{13}C NMR data. The electronic structure was analyzed in terms of the interactions between the frontier orbitals of the metal fragment and of the butadiene unit (see Figure 10). The orbitals of the [calix[4]-$(OMe)(O)_3$Ta] fragment are reported in the second column of Figure 6. For such a Ta^{II} fragment with a d^2 electron count, the lowest, almost degenerate, 1a′ and 2a′ orbitals are occupied by two electrons. On the extreme right of Figure 10 we show the frontier orbitals of butadiene, that is the four π and π* orbitals. The

0947-6539/99/0502-0730 $ 17.50+.50/0 *Chem. Eur. J.* **1999**, *5*, No. 2

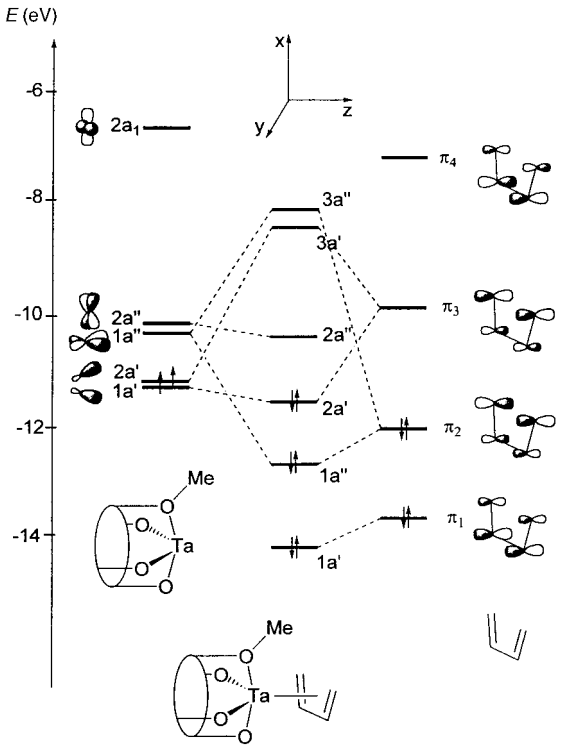

Figure 10. Orbital interaction diagram for [Ta{calix[4]-(OMe)(O)$_3$}(η^4-C_4H_6)].

interaction between the [calix[4]-(OMe)(O)$_3$Ta] fragment and the butadiene moiety is illustrated by the molecular orbital diagram for **25** in the central column of Figure 10. Two significant interactions can be seen from Figure 10: the empty 1a″(d_{yz}) interacts with the occupied π_2-orbital, while the occupied 1a′ and 2a′ match with the empty π_3* and produce the HOMO of the complex. The former interaction is of the donation type while the latter describes the back-donation from the metal to butadiene. These interactions are similar to those observed in the [Fe(CO)$_3$(butadiene)] complex[19] and lead to an analogous π^2,η^4-bonding mode with all four carbon atoms of butadiene almost equally involved in the metal–butadiene bond. This is confirmed by the overlap populations calculated for **25** and compared, in Table 4, with the reported values for the [Fe(CO)$_3$(butadiene)] and [Cp$_2$Zr(butadiene)] complexes.[19] We see that in **25** all four Ta–C bonds show the same bond strength and that also the C_1-C_2 and C_2-C_3 bonds are equally strong.

The π^2-coordination mode of butadiene in **25** is different from the σ^2-π metallacyclopentene structure observed in [Cp$_2$Zr(butadiene)] (***E*** in Scheme 5) and in other butadiene complexes of electropositive, early transition metals.[20] This seemingly surprising difference is easily explained on the basis of the different frontier orbitals of the [calix[4]-(OMe)(O)$_3$Ta] and [Cp$_2$Zr] metal fragments. In the [Cp$_2$Zr] fragment, only one d_π orbital, 1b$_2$(d_{yz}), is available for the donation from π_2, and the back-donation is described by 1a$_1$-π_3* mixing (Scheme 6) which, as a result of the higher components on the outer carbon in π_3*, involves mainly the two terminal carbon atoms.[19] Instead, in **25** a second d_π orbital (the d_{xz} spread in 1a′ and 2a′) is available for the back-donation to π_3* and all four carbon atoms are involved in this interaction (Scheme 6).

Table 4. Comparison of the calculated overlap populations in **25** with those for [Cp$_2$Zr(butadiene)] and [Fe(CO)$_3$(butadiene)].[19]

	25	[Fe(CO)$_3$(butadiene)]	[Cp$_2$Zr(butadiene)]
M–C$_1$	0.233	0.202	0.338
M–C$_2$	0.196	0.184	0.060
C$_1$–C$_2$	0.994	0.979	0.991
C$_2$–C$_3$	0.941	0.974	1.012

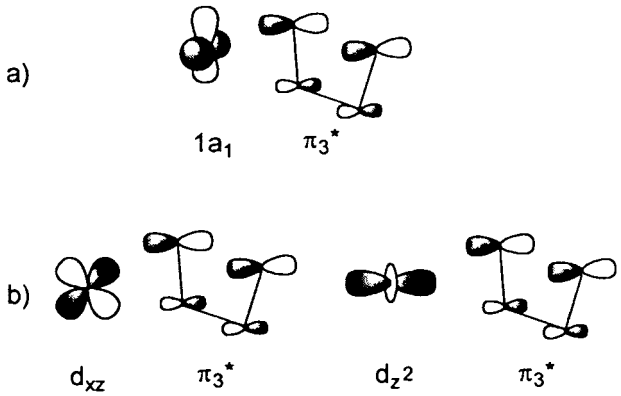

Scheme 6. Back-bonding in the [Cp$_2$Zr] fragment (a) and in complex **25** (b).

Figure 10 illustrates that a low-lying orbital of d_{z^2} character, mixed with d_{xz} in the 1a′ and 2a′ orbitals, is also available for the [calix[4]-(OMe)(O)$_3$Ta] fragment so that a d_{z^2}-π_3* interaction would be expected for **25** (Scheme 6) which would lead to a σ^2-π character. In order to study this point, we performed EH calculations on **25** in which the dihedral angle θ was progressively increased from 15° (the optimal value for the π^2 structure) to 30°, which is a typical value for a σ^2-π geometry. A small increase in energy was observed, and the σ^2-π structure was calculated to be only $\approx$10 kcal mol^{-1} higher than that for the optimal π^2 structure. Moreover, an analysis of the molecular orbitals shows that as θ increases, the HOMO shifts continuously from a d_{xz}-π_3* to a d_{z^2}-π_3* character to reach a mainly d_{z^2}-π_3* configuration in the final σ^2-π geometry. In other words, the two low-lying, almost degenerate, 1a′ and 2a′ orbitals of [calix[4]-(OMe)(O)$_3$Ta] are combinations of the d_{xz} and d_{z^2}, whose back-donation to the π_3* orbital of butadiene leads, respectively, to a π^2 or a σ^2-π structure. The observed preference for the former structure is probably determined by the better d_{xz}-π_3* overlap, but the σ^2-π structure is easily available and may play an important role in the peculiar reactivity pattern of this butadiene complex.

Although no X-ray analysis could be performed on **25**, some structural information was obtained from the NMR spectra (vide infra) which suggests that the plane bisecting the butadiene lies in the *xz* plane which contains the methoxy group of the calix[4]arene ligand. This orientation (***F*** in Scheme 5) is analogous to that observed for the structurally characterized [calix[4]-(OMe)$_2$(O)$_2$Zr(butadiene)] compounds in which the plane bisecting the butadiene lies in the

xz plane that contains the two methoxy groups of the calix[4]arene ligand. This orientation is determined by the more favorable interaction of the butadiene π_2 and π_3* orbitals with the two d_π orbitals of the [calix[4]-$(OMe)(O)_3$-Ta)] fragment, and also leads to a lower steric repulsion between the butadiene and the methoxy group of the calix[4]arene ligand. The alternative orientation with the plane bisecting the butadiene in the orthogonal yz plane (***G*** in Scheme 5) has been calculated, with reoptimization of *R*, *L*, and θ, and is $\approx$35 kcal mol^{-1} higher in energy, which suggests that butadiene rotation does not occur at room temperature. The ^{13}C NMR data indicate that the bonding of the diene ligand has a mainly η^4,π^2 character rather than a η^4,σ^2-π character. Indeed, the $^{13}C-^{1}H$ coupling constant observed for the terminal CH_2 in **25** ($J = 151$ Hz) is only slightly smaller than the usual values for the hybridized sp^2 carbon atoms ($J =$ 155–160 Hz); this indicates a small amount of rehybridization of the diene methylene group towards sp^3 hybridization. The observed J_{CH} is significantly higher that the usual value for a sp^3-hybridized carbon atom ($J = 125$ Hz) and application of Newton's semiempirical equation[21] allows a rough estimate of $n = 2.2$ for the extent of spin hybridation for the methylene carbons in **25**. The ^{1}H and ^{13}C NMR (200 MHz) spectra of **25** revealed a fluxional character of the diene–tantalum bond above $-60\,^\circ$C. In the spectrum at room temperature the terminal butadiene protons are in equilibrium and show only one doublet at $\delta = 2.69$. Only one multiplet at $\delta = 6.45$ is observed for the two protons of the *meso* carbons. This pattern did not change when the temperature was lowered, and only a partial splitting into two groups, assignable to *syn* and *anti* protons at the butadiene termini, could be observed at the lowest measured temperature of $-60\,^\circ$C. The interconversion of the terminal protons in **25** could be explained by the envelope flipping of the butadiene ligand through a planar metallacyclopentene transition state (Scheme 7). This mechanism has been investigated by the calculation of the relative

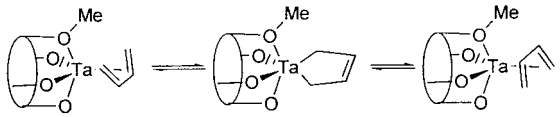

Scheme 7. Rearranging modes of butadiene over a Ta–monomethoxy calix[4]arene moiety.

energy of the postulated planar metallacyclopentene transition state. The geometry of this species has been optimized by variation of the distance *R* between tantalum and the C_1-C_4 line (***H*** in Scheme 5); the results indicate an energy barrier of $\approx$16 kcal mol^{-1}, which is compatible with the observed ^{1}H NMR behavior.

Useful structural information on the molecular symmetry of **25** can be deduced from the ^{1}H NMR data: complex **25** exhibits a C_s symmetry, as evidenced by its ^{1}H NMR spectrum which shows two pairs of doublets ($\delta = 3.18$, 4.22, and 3.28, 4.54 at 30 °C) for the bridging methylene protons. This pattern did not change when the temperature was lowered, which indicates that **25** maintains its C_s symmetry at $-60\,^\circ$C. This behavior suggests that the coordination geometry of the butadiene, with its bisecting plane lying in the *xz* plane containing the methoxy group of the calix[4]arene ligand (***F*** in Scheme 5), is favored over the alternative orthogonal geometry (***G*** in Scheme 5) which would give a C_1 geometry and even account for the flipping process (see above). This is in agreement with our extended Hückel calculations (see above), which indicate for ***G*** a much higher energy than ***F*** (35 kcal mol^{-1}).

Conclusions

The organometallic chemistry of tantalum(v) bonded over an oxo-matrix was illustrated by the calix[4]arene-tantalum(v) fragments. A number of relevant results were obtained:

1) The acid-base chemistry of the metal is synergic with the cleavage of the C–O bond and leads to the demethylation of methoxy groups on a calix[4]arene skeleton. In some cases this can be an interesting synthetic route to otherwise inaccessible anionic forms of η^2-acyls and η^2-iminoacyls. The extended Hückel calculations enabled discrimination between metal-assisted and non-metal-assisted processes.
2) The migratory insertion reactions of CO and RNC with $[TaR_2]$ fragments led exclusively to the formation of the η^2-ketone or the η^2-imine, respectively, without the possibility of intercepting the corresponding η^2-acyls or η^2-iminoacyl. Such a result is in agreement with a facial rather than a meridional (see Cp_2Zr fragments) arrangement of the three frontier orbitals involved in the process.
3) When the formation of a η^2-ketone or η^2-imine is prevented, the [Ta–R] functionality (see complexes **6**–**8**) does not undergo any migratory insertion reaction. In such cases the reversible precoordination of *t*BuNC was observed.

A quite rare example of a tantalum(v)–butadiene functionality, bound over an oxo-matrix, was reported. Although butadiene displays an essentially η^4,π^2-bonding mode, the Ta–butadiene complexes behave either similarly to diallyl derivatives in insertion reactions, as expected for a η^4,σ^2-π-bonding mode of the butadiene, or similarly to a source of tantalum(III)-d^2 carbenoid fragment, depending on the nature of the substrate.

Experimental Section

General procedure: All reactions were carried out under an atmosphere of purified nitrogen. Solvents were dried and distilled before use by standard methods. ^{1}H NMR and IR spectra were recorded on Bruker AC200, DPX400, and Perkin–Elmer FT1600 instruments, respectively. GC and GC-MS analyses were carried out with a HP5890 Series II system and a HP5890AGC system, respectively. The synthesis of [*p*-*t*Bu-calix[4]-$(OMe)_2(OH)_2$] (**2**) was performed as reported in the literature.[22]

Synthesis of 3: $TaCl_5$ (18.55 g, 51.8 mmol) was added to a suspension of **1**·CH_2Cl_2 (38.06 g, 51.8 mmol) in toluene (500 mL) at room temperature. The mixture was heated to reflux for 14 h, then volatiles were removed in a vacuum, and toluene was added to the yellow residue that was collected and dried in a vacuum. Yield: 43.20 g (85%); ^{1}H NMR (CD_2Cl_2, 298 K): $\delta = 7.22$ (m, 13H; arom), 5.11 (d, $J = 12.4$ Hz, 2H; CH_2-calix), 4.59 (d, $J =$ 13.6 Hz, 2H; CH_2-calix), 3.53 (d, $J = 12.4$ Hz, 2H; CH_2-calix), 3.4 (d, $J =$ 13.6 Hz, 2H; CH_2-calix). 2.34 (s, 3H; CH_3-toluene), 1.33 (s, 9H; *t*Bu-calix),

0947-6539/99/0502-0732 $ 17.50+.50/0 *Chem. Eur. J.* **1999**, *5*, No. 2

1.24 (s, 18H; *t*Bu-calix), 1.18 (s, 9H; *t*Bu-calix); anal. calcd for $\mathbf{3}\cdot 2C_7H_8$, $C_{102}H_{120}Cl_2O_8Ta_2$ (1906.87): C 64.25, H 6.34; found: C 64.54, H; 6.31.

Synthesis of 4: $TaCl_5$ (20.95 g, 58.5 mmol) was added to a solution of **2** (39.2 g, 57.9 mmol) in toluene (400 mL). The mixture was refluxed for 36 h, then volatiles were removed in a vacuum, and the yellow residue was washed with *n*-hexane (200 mL), collected, and dried in a vacuum. Yield: 43.23 g (74%). Crystals suitable for X-ray analysis were grown from a saturated solution in toluene and *n*-hexane at room temperature. ^{1}H NMR (C_6D_6, 298 K): $\delta = 7.00$ (m, 13H; arom), 4.97 (d, $J = 13.8$ Hz, 2H; CH_2-calix), 4.36 (d, $J = 13.3$ Hz, 2H; CH_2-calix), 3.95 (s, 3H; OCH_3), 3.30 (d, $J = 13.8$ Hz, 2H; CH_2-calix), 3.15 (d, $J = 13.3$ Hz, 2H; CH_2-calix), 2.10 (s, 3H; CH_3-toluene), 1.34 (s, 18H; *t*Bu-calix), 0.73 (s, 9H; *t*Bu-calix), 0.67 (s, 9H; *t*Bu-calix); anal. calcd for $\mathbf{4}\cdot C_7H_8$, $C_{52}H_{63}Cl_2O_4Ta$ (1003.92): C 62.21, H 6.32; found: C 61.78, H 6.12. A sample of the product in C_5D_5N gave complex **5**, as shown by the NMR spectrum: ^{1}H NMR (C_5D_5N, 298 K): $\delta =$ 7.55 (m, 8H; arom), 5.30 (d, $J = 12.7$ Hz, 4H; CH_2-calix), 4.10 (s, 3H; CH_3-N), 3.53 (d, $J = 12.7$, 4H; CH_2-calix), 1.40 (s, 18H; *t*Bu), 0.79 (s, 18H; *t*Bu).

Synthesis of 5: Pyridine (10 mL) was added to a yellow solution of $\mathbf{4}\cdot C_7H_8$ (2.00 g, 1.99 mmol) in toluene (100 mL). After 12 h the solution gave a suspension of white solid which was collected and dried in a vacuum. Yield: 1.4 g (68%); ^{1}H NMR (C_5D_5N, 298 K): $\delta = 8.85$ (d, $J = 5.87$ Hz, 2H; pyridine), 8.27 (t, $J = 7.8$ Hz, 1H; pyridine), 7.73 (m, 2H; pyridine), 7.48 (s, 4H; arom-calix), 7.26 (m, 2.5H; tol), 7.09 (s, 4H; arom-calix), 5.32 (d, $J =$ 12.8 Hz, 4H; CH_2-calix), 4.17 (s, 3H; CH_3-N), 3.52 (d, $J = 12.7$ Hz, 4H; CH_2-calix), 2.2 (s, 1.5H; CH_3-tol), 1.34 (s, 18H; *t*Bu), 0.82(s, 18H; *t*Bu); anal. calcd. for $\mathbf{5}\cdot 0.5\,C_7H_8$, $C_{53.5}H_{64}Cl_2NO_4Ta$ (1036.95): C 61.97, H; 6.22, N 1.35; found: C 61.98, H 6.11, N 1.45.

Synthesis of 7: A solution of $(PhCH_2)_2Mg$ (0.17 M, 3.06 mmol) in THF (18 mL) was added dropwise to a suspension of $\mathbf{3}\cdot 2C_7H_8$ (5.84 g, 3.06 mmol) in benzene (200 mL). The yellow suspension was heated to reflux for 1 h, yielding a brown suspension. Dioxane (2 mL) was added to the reaction mixture, then volatiles were removed in a vacuum, and the solid residue was extracted with benzene (300 mL). The solvent was then evaporated to dryness, and the residue washed with *n*-hexane (60 mL) and collected as a white powder. Yield: 2.33 g (42%). Crystals suitable for X-ray analysis were grown from a saturated benzene and *n*-hexane solution at room temperature. ^{1}H NMR (C_6D_6, 298 K): $\delta = 7.43$ (d, $J = 8.2$ Hz, 2H; arom), 7.23 (m, 2H; arom), 7.06 (s, 8H; arom-calix), 6.91 (t, $J = 7.2$ Hz, 1H; arom), 4.98 (d, $J = 12.2$ Hz, 4H; CH_2-calix), 3.62 (s, 2H; CH_2-Bn), 3.28 (d, $J = 12.2$ Hz, 4H; CH_2-calix), 1.09 (s, 36H; *t*Bu-calix) corresponds to the monomeric form **7b**. ^{1}H NMR (CD_2Cl_2, 298 K): $\delta = 7.39$ (m, 5H; arom), 7.12 (s, 8H; arom), 4.69 (d, $J = 12.2$ Hz, 4H; CH_2-calix), 3.79 (s, 2H; CH_2Ph), 3.34 (d, $J = 12.2$ Hz, 4H; CH_2-calix), 1.19 (s, 36H; *t*Bu-calix); anal. calcd. for $C_{102}H_{118}O_8Ta_2$ (1833.95): C 66.80, H 6.49; found: C 66.66, H 6.68. A stoichiometric amount of *t*BuNC was added to a sample of **7** in toluene. The reaction was followed by IR and ^{1}H NMR spectroscopy. The IR spectrum showed the presence of two characteristic peaks: $\tilde{\nu} = 2133$ cm^{-1} (free *t*BuNC) and 2169.2 cm^{-1} (coordinated *t*BuNC). The NMR spectra in CD_2Cl_2 showed broad peaks for *endo*-CH_2 of calix[4]arene, CH_2Ph, and coordinated *t*BuNC (at $\delta = -0.26$). Upon the addition of excess *t*BuNC, the NMR signals for *endo*-CH_2 and CH_2Ph shifted and became sharper. The peak of coordinated *t*BuNC became sharper at low temperature (263 K). ^{1}H NMR (CD_2Cl_2, 263 K): $\delta = 7.39$ (d, $J = 8$ Hz, 2H; arom), 7.31 (m, 2H; arom), 7.18 (s, 8H; arom-calix), 6.95 (t, $J = 8$ Hz, 1H; arom), 4.76 (d, $J =$ 12 Hz, 4H; CH_2-calix), 3.36 (d, $J = 12$ Hz, 4H; CH_2-calix), 3.25 (s, 2H; CH_2Ph), 1.42 (s, free *t*BuNC), 1.18 (s, 18H; *t*Bu-calix), -0.33 (s, 9H; coordinated *t*BuNC).

Synthesis of 8: A solution of *p*-MeC_6H_4MgBr (0.8 M, 6.05 mmol) in THF (7.6 mL) was added dropwise to a suspension of $\mathbf{3}\cdot 2C_7H_8$ (5.77 g, 3.02 mmol) in THF (100 mL). The yellow suspension was heated to reflux for 12 h. Dioxane (3 mL) was added to the reaction, then the volatiles were removed in a vacuum, and the solid residue was extracted with benzene (300 mL). The solvent was then evaporated to dryness, the solid residue washed with *n*-hexane (60 mL), and then collected. Yield: 2.5 g (45%). A mixture of **8a** and **8b** was detected in the ^{1}H NMR spectrum: ^{1}H NMR (dimeric form **8a**) (C_6D_6, 298 K): $\delta = 8.33$ (d, $J = 7.32$ Hz, 2H; arom), 7.37 (d, $J = 2$ Hz, 2H; arom), 7.24 (d, $J = 2$ Hz, 2H; arom), 6.89 (s, 2H; arom), 6.78 (s, 2H; arom), 6.75 (d, $J = 7.32$ Hz, 2H; arom), 5.94 (d, $J = 12.2$ Hz, 2H; CH_2-calix), 5.32 (d, $J = 13.18$ Hz, 2H; CH_2-calix), 3.49 (d, $J = 12.2$ Hz, 2H; CH_2-calix), 3.41 (d, $J = 13.18$ Hz, 2H; CH_2-calix), 1.78 (s, 3H; CH_3-*p*-tol), 1.27 (s, 18H; *t*Bu), 1.00 (s, 9H; *t*Bu), 0.93 (s, 9H; *t*Bu); ^{1}H NMR (monomeric form **8b**) (C_6D_6, 298 K): $\delta = 8.64$ (d, $J = 7.80$ Hz, 2H; arom), 7.24 (m, 10H; arom), 5.15 (d, $J = 12.2$ Hz, 4H; CH_2-calix), 3.35 (d, $J =$ 12.2 Hz, 4H; CH_2-calix), 2.04 (s, 3H; CH_3-*p*-tol), 1.13 (s, 36H; *t*Bu-calix); anal. calcd. for $C_{102}H_{118}O_8Ta_2$ (1833.95): C 66.80, H 6.49; found: C 66.48, H 6.55. A sample of the product heated in C_5D_5N gave only the monomeric species: ^{1}H NMR (C_5D_5N, 298 K): 8.46 (d, $J = 7.82$ Hz, 2H; arom), 7.4 (m, 10H; arom), 4.98 (d, $J = 12.2$ Hz, 4H; CH_2-calix), 3.55 (d, $J = 12.2$ Hz, 4H; CH_2-calix), 2.08 (s, 3H; CH_3-*p*-tol), 1.12 (s, 36H; *t*Bu).

Synthesis of 9: A solution of MeLi (1.12 M, 12.15 mmol) in diethyl ether (10.84 mL) was added dropwise to a yellow solution of $\mathbf{4}\cdot C_7H_8$ (6.10 g, 6.07 mmol) in toluene (300 mL) at $-10\,^\circ$C. The mixture was refluxed for 12 h to give a dark suspension. Volatiles were removed in a vacuum and the solid residue was extracted with diethyl ether (300 mL). The solvent was evaporated to dryness, the residue dissolved in *n*-hexane (60 mL), and the mixture was kept at $-30\,^\circ$C for 6 days to yield a white precipitate that was collected and dried in a vacuum. Yield: 2.7 g (46%); ^{1}H NMR (C_5D_5N, 298 K): $\delta = 7.44$ (d, $J = 2.44$ Hz, 2H; arom), 7.31 (d, $J = 2.44$ Hz, 2H; arom), 6.90 (s, 2H; arom), 6.68 (s, 2H; arom), 4.92 (d, $J = 13.18$ Hz, 2H; CH_2-calix), 4.31 (d, $J = 13.18$ Hz, 2H; CH_2-calix), 3.79 (s, 3H; OCH_3), 3.49 (d, $J = 13.18$ Hz, 2H; CH_2-calix), 3.28 (d, $J = 13.18$ Hz, 2H; CH_2-calix), 1.47 (s, 6H; CH_3), 1.40 (s, 18H; *t*Bu), 1.17 (m, 8H; hexane), 1.06 (s, 9H; *t*Bu), 0.83 (s, 9H; *t*Bu), 0.82 (m, 6H; hexane); ^{1}H NMR (C_6D_6, 298 K): $\delta = 7.23$ (s, 4H; arom), 6.86 (s, 2H; arom), 6.83 (s, 2H; arom), 4.88 (d, $J = 13.16$ Hz, 2H; CH_2-calix), 4.36 (d, $J = 12.7$, 2H; CH_2-calix), 3.54 (s, 3H; OCH_3), 3.34 (d, $J = 13.16$, 2H; CH_2-calix), 3.19 (d, $J = 12.7$, 2H; CH_2-calix), 1.79 (s, 6H; CH_3), 1.39 (s, 18H; *t*Bu), 1.23 (m, 8H; hexane), 0.88 (m, 6H; hexane), 0.80 (s, 9H; *t*Bu), 0.71 (s, 9H; *t*Bu); anal. calcd for $\mathbf{9}\cdot C_6H_{14}$, $C_{53}H_{75}O_4Ta$ (973.12): C 66.50, H 7.91; found: C 66.33, H 7.56. Complex **9** is thermally stable in solution. A sample of **9** heated in C_5D_5N at 90 °C for 24 h gave a mixture of **6a** and **6b**, which we were unable to synthesize from **3**. ^{1}H NMR (**6a**) (C_5D_5N, 298 K): $\delta = 7.34$ (m, 8H; arom-calix), 5.79 (d, $J = 12.2$ Hz, 2H; CH_2-calix), 4.55 (d, $J = 13.66$ Hz, 2H; CH_2-calix), 3.89 (d, $J = 12,2$ Hz, 2H; CH_2-calix), 3.65 (d, $J = 13.66$ Hz, 2H; CH_2-calix), 1.41 (s, 3H; CH_3), 1.28 (s, 18H; *t*Bu), 1.25 (s, 9H; *t*Bu), 1.21 (s, 9H; *t*Bu); ^{1}H NMR (**6b**) (C_5D_5N, 298 K): $\delta = 7.34$ (m, 8H; arom-calix), 4.88 (d, $J = 12.2$ Hz, 4H; CH_2-calix), 3.53 (d, $J = 12.2$ Hz, 4H; CH_2-calix), 1.42 (s, 3H; CH_3), 1.12 (s, 36H; *t*Bu).

Synthesis of 10: A solution of $(PhCH_2)_2Mg$ (0.34 M, 3.73 mmol) in THF (10.96 mL) was added dropwise to a yellow solution of $\mathbf{4}\cdot C_7H_8$ (3.74 g, 3.73 mmol) in toluene (150 mL). The mixture became orange in seconds, and dioxane (6 mL) was added after 15 min. The reaction mixture was stirred for 1 h, the salts were filtered off, and the volatiles were removed in a vacuum. The yellow residue was washed with *n*-hexane (70 mL), collected, and dried in a vacuum. Yield: 1.6 g (42%); ^{1}H NMR (C_6D_6, 298 K): $\delta = 7.16$ (m, 18H; arom), 4.44 (d, $J = 13.2$ Hz, 2H; CH_2-calix), 4.31 (d, $J = 13.3$ Hz, 2H; CH_2-calix), 3.60 (brs, 4H; CH_2-Ph), 3.23 (d, $J =$ 12.6 Hz, 2H; CH_2-calix), 3.19 (s, 3H; OCH_3), 3.12 (d, $J = 13.3$ Hz, 2H; CH_2-calix), 1.39 (s, 18H; *t*Bu), 0.72 (s, 9H; *t*Bu), 0.67 (s, 9H; *t*Bu); anal. calcd for $C_{59}H_{69}O_4Ta$ (1023.14): C 69.26, H 6.80; found: C 69.35, H 7.10. The product is thermally stable in solution (benzene, 100 °C, 24 h), but it is photosensitive: a sample of **10** exposed to visible light in benzene over 24 h gave 1,2-diphenylethane and **7**, while heated at 80 °C in pyridine it gave **7** and a mixture of 2-benzylpyridine and 4-benzylpyridine (GC-MS). The same transformation of **10** into **7** occurs in the presence of H_2 (1 atm) in benzene.

Synthesis of 11: A solution of *p*-MeC_6H_4MgBr (0.98 M, 6.25 mmol) in THF (6.4 mL) was added dropwise to a yellow solution of $\mathbf{4}\cdot C_7H_8$ (3.13 g, 3.12 mmol) in toluene (150 mL). After 20 min, dioxane (6 mL) was added to the reaction mixture. Salts were filtered off. The solvent was evaporated to dryness and the gray-yellow residue was washed with *n*-hexane (70 mL) and collected. Yield: 1.59 g (50%); ^{1}H NMR (C_6D_6, 298 K): $\delta = 8.37$ (d, $J =$ 7.60 Hz, 4H; arom), 7.30 (d, $J = 2.2$ Hz, 2H; arom), 7.28 (d, $J = 2.2$ Hz, 2H; arom), 7.14 (d, $J = 7.60$ Hz, 4H; arom), 6.87 (s, 2H; arom), 6.81 (s, 2H; arom), 4.95 (d, $J = 13.2$ Hz, 2H; CH_2-calix), 4.6 (d, $J = 12.5$ Hz, 2H; CH_2-calix), 3.65 (s, 3H; OCH_3), 3.29 (d, $J = 12.5$ Hz, 4H; CH_2-calix), 2.12 (s, 6H; CH_3-*p*-tol), 1.37 (s, 18H; *t*Bu), 0.77 (s, 9H; *t*Bu), 0.71 (s, 9H; *t*Bu); anal. calcd for $C_{59}H_{69}O_4Ta$ (1023.14): C 69.26, H; 6.80; found: C 69.32, H 7.17. The solution of **11** in toluene is quite thermally stable, though it very slowly forms a mixture containing **8**. Complex **11**, heated to 80 °C for 2 h in C_5D_5N, gave quantitatively **8** and 4,4′-dimethylbiphenyl (GC-MS).

Synthesis of 12: A solution of MeLi (1.76 M, 7.5 mmol) in diethyl ether (4.29 mL) was added dropwise to a yellow solution of $\mathbf{4}\cdot C_7H_8$ (3.77 g,

3.75 mmol) in toluene (200 mL). Refluxing this mixture for 12 h resulted in a dark suspension, which was filtered to remove the salts, and then saturated with CO. After 2 h, the solvent was evaporated to dryness, and the residue dissolved in *n*-hexane (60 mL). The product was very soluble and could not be isolated. ^{1}H NMR (C_5D_5N, 298 K): $\delta = 6.96$ (m, 8H; arom), 4.98 (d, $J = 12.20$ Hz, 2H; CH_2-calix), 4.36 (s, 3H; OCH_3), 4.21 (d, $J = 12.20$ Hz, 2H; CH_2-calix), 3.28 (d, $J = 12.2$ Hz, 2H; CH_2-calix), 3.10 (d, $J = 12.2$ Hz, 2H; CH_2-calix), 2.79 (s, 6H; CH_3), 1.39 (s, 18H; *t*Bu), 0.85 (s, 9H; *t*Bu), 0.68 (s, 9H; *t*Bu).

Synthesis of 13: A solution of **10** (2.34 g, 2.28 mmol) in toluene (120 mL) was saturated with CO. The mixture was stirred at room temperature for 2 h to give a yellow solution. The solvent was removed in a vacuum and the yellow residue was dissolved in *n*-hexane (50 mL), filtered, and kept at $-30\,^\circ$C for 12 h to yield a white precipitate that was collected. Yield: 1.37 g (57%). Crystals suitable for X-ray analysis were obtained by cooling a saturated solution in *n*-hexane/benzene (10:1) from room temperature to 2 °C. ^{1}H NMR (C_6D_6, 298 K): $\delta = 7.70$ (d, $J = 8.28$ Hz; 4H; arom), 7.02 (m; 14H; arom), 4.94 (d, $J = 12.50$ Hz, 2H; CH_2-calix), 4.42 (d, $J = 14.70$ Hz, 2H; CH_2Ph), 4.32 (s, 3H; OCH_3), 4.15 (d, $J = 14.7$ Hz, 2H; CH_2Ph), 4.06 (d, $J = 12.50$ Hz, 2H; CH_2-calix), 3.26 (d, $J = 12.50$ Hz, 2H; CH_2-calix), 3.10 (d, $J = 12.50$ Hz, 2H; CH_2-calix), 1.38 (s, 18H; *t*Bu), 0.83 (s, 9H; *t*Bu), 0.67 (s, 9H; *t*Bu); anal. calcd for $C_{60}H_{69}O_5Ta$ (1051.15): C 68.56, H 6.62; found: C 68.62, H 7.33. The product is thermally and photochemically stable in solution. A sample heated to 80 °C in C_5D_5N gave **18** quantitatively: ^{1}H NMR (C_5D_5N, 298 K): $\delta = 7.83$ (d, $J = 8$ Hz; 4H; arom), 7.19 (m, 14H; arom), 5.23 (d, $J = 11.72$ Hz, 4H; CH_2-calix), 4.49 (d, $J = 15.14$ Hz, 2H; CH_2-Bn), 4.42 (s, 3H; H_3C-N), 4.05 (d, $J = 15.14$ Hz, 2H; CH_2-Bn), 3.4 (d, $J = 11.72$ Hz, 4H; CH_2-calix), 1.2 (s, 36H; *t*Bu).

Synthesis of 14: A solution of **11** (2.94 g, 2.87 mmol) in toluene (120 mL) was saturated with CO. The mixture was stirred at room temperature for 3 h to give a yellow solution. The solvent was evaporated to dryness. Diethyl ether was added to the yellow residue and the mixture was filtered. The solvent was removed in a vacuum and the yellow residue was washed with *n*-hexane (50 mL) and then collected. Yield: 1.50 g (50%); ^{1}H NMR (C_6D_6, 298 K): $\delta = 8.20$ (d, $J = 8.20$ Hz, 4H; arom), 7.24 (s, 2H; arom), 7.20 (s, 2H; arom), 7.08 (d, $J = 2.35$ Hz, 2H; arom), 7.03 (d, $J = 2.35$ Hz; 2H; arom), 6.81 (d, $J = 8.20$ Hz, 4H; arom), 4.69 (d, $J = 12.44$ Hz, 2H; CH_2-calix), 4.48 (s, 3H; OCH_3), 4.16 (d, $J = 12.44$ Hz, 2H; CH_2-calix), 3.09 (d, $J = 12.58$ Hz, 2H; CH_2-calix), 3.03 (d, $J = 12.58$ Hz, 2H; CH_2-calix), 2.17 (s, 6H; CH_3-*p*-tol), 1.30 (s, 18H; *t*Bu), 0.79 (s, 9H; *t*Bu), 0.66 (s, 9H; *t*Bu); anal. calcd for $C_{60}H_{69}O_5Ta$ (1051.15): C 68.56, H 6.62; found: C 68.29, H 6.99.

Synthesis of 15: *t*BuNC (0.27 g, 3.30 mmol) was added to a stirred solution of **9** · C_6H_{14} (3.16 g, 3.30 mmol) in benzene (120 mL). After 10 h the mixture was filtered. The solvent was removed in a vacuum and the brown residue dissolved in *n*-hexane (60 mL), filtered, and kept at $-30\,^\circ$C for 6 days to yield a light gray precipitate that was collected. Yield: 1.5 g (44%); ^{1}H NMR (C_6D_6, 298 K): $\delta = 7.23$ (d, $J = 2.44$ Hz, 2H; arom), 7.20 (d, $J = 2.44$ Hz, 2H; arom), 6.86 (s, 2H; arom), 6.82 (s, 2H; arom), 4.98 (d, $J = 12.2$ Hz, 2H; CH_2-calix), 4.32 (d, $J = 12.2$ Hz, 2H; CH_2-calix), 4.18 (s, 3H; OCH_3), 3.25 (d, $J = 12.2$ Hz, 2H; CH_2-calix), 3.21 (d, $J = 12.2$ Hz, 2H; CH_2-calix), 2.38 (s, 6H; CH_3), 1.98 (s, 9H; *t*BuN), 1.40 (s, 18H; *t*Bu), 1.23 (m, 8H; hexane), 0.88 (m, 6H; hexane), 0.85 (s, 9H; *t*Bu), 0.70 (s, 9H; *t*Bu); anal. calcd for **15** · C_6H_{14}, $C_{58}H_{84}NO_4Ta$ (1040.26): C 66.97, H 8.14, N 1.34; found: C 66.84 H 7.86, N 1.14.

Synthesis of 16: *t*BuNC (0.14 g ,1.68 mmol) was added to a stirred solution of **10** (1.72 g, 1.68 mmol) in benzene (120 mL). After 12 h the solvent was removed in a vacuum and the yellow residue was dissolved in *n*-hexane (60 mL), filtered, and then kept at $-30\,^\circ$C for 6 days to give a light yellow precipitate that was collected. Yield: 1.00 g (50%); ^{1}H NMR (C_6D_6, 298 K): $\delta = 7.54$ (d, $J = 6.84$ Hz, 4H; arom), 7.10 (m; 10H; arom), 6.84 (s, 2H; arom), 6.74 (s, 2H; arom), 5.06 (d, $J = 12.7$ Hz, 2H; CH_2-calix), 4.24 (d, $J = 14.16$ Hz, 2H; CH_2Ph), 4.08 (d, $J = 14.16$ Hz, 2H; CH_2Ph), 3.84 (d, $J = 12.7$ Hz, 2H; CH_2-calix), 3.47 (s, 3H; OCH_3), 3.31 (d, $J = 12.2$ Hz, 2H; CH_2-calix), 2.95 (d, $J = 12.2$ Hz, 2H; CH_2-calix), 2.05 (s, 9H *t*BuN), 1.39 (s, 18H; *t*Bu), 1.23 (m, 8H; hexane), 0.88 (m, 6H; hexane), 0.86 (s, 9H; *t*Bu), 0.68 (s, 9H; *t*Bu); anal. calcd for **16** · C_6H_{14}, $C_{70}H_{92}NO_4Ta$ (1192.45): C 70.51, H 7.78, N 1.17; found: C 70.79, H 7.85, N 1.21. The product is thermally and photochemically stable in solution. A sample in C_5D_5N for 24 h gave **19** quantitatively: ^{1}H NMR (C_5D_5N, 298 K): $\delta = 7.89$ (d, $J = 6.84$ Hz, 4H; arom), 7.19 (m, 14H; arom), 5.20 (d, $J = 11.72$ Hz, 4H; CH_2-calix), 4.82 (d, $J = 15.62$ Hz, 2H; CH_2-Bn), 4.47(d, $J = 15.62$ Hz, 2H; CH_2-Bn), 3.40 (s, 3H; H_3C-N), 3.32 (d, $J = 11.72$ Hz, 4H; CH_2-calix), 1.94 (s, 9H; *t*BuNC), 1.15 (s, 36H; *t*Bu).

Synthesis of 17: A solution of *t*BuNC (0.17 g, 2.08 mmol) in toluene (20 mL) was added dropwise by to a stirred solution of **11** (2.13 g, 2.08 mmol) in toluene (100 mL). After 2 h the solvent was removed in a vacuum and diethyl ether (100 mL) was added to the yellow residue. The ethereal solution was filtered, the solvent removed in a vacuum, the residue washed with *n*-hexane (70 mL), and collected. Yield: 1.06 g (46%); ^{1}H NMR (C_6D_6, 298 K): $\delta = 7.98$ (d, $J = 8.2$ Hz; 4H; arom), 7.25 (d; $J = 2.3$ Hz, 2H; arom), 7.14 (d, $J = 2.3$ Hz, 2H; arom), 7.05 (d, $J = 8.2$ Hz, 4H; arom), 6.86 (s, 2H; arom), 6.76 (s, 2H; arom), 5.20 (d, $J = 12.34$ Hz, 2H; CH_2-calix), 4.24 (s, 3H; OCH_3), 4.14 (d, $J = 12.34$ Hz, 2H; CH_2-calix), 3.35 (d, $J = 12.5$ Hz, 2H; CH_2-calix), 3.11 (d, $J = 12.5$ Hz, 2H; CH_2-calix), 2.19 (s, 6H; CH_3*p*-tol), 1.94 (s, 9H; *t*BuN), 1.36 (s, 18H; *t*Bu), 0.87 (s, 9H; *t*Bu), 0.61 (s, 9H; *t*Bu); anal. calcd for $C_{64}H_{78}NO_4Ta$ (1106.28): C 69.49, H 7.11, N 1.27; found: C 69.46, H 7.26, N 1.12. The product is thermally and photochemically stable in solution. A sample of **17** heated at 80 °C for 24 h in C_5D_5N gave **20** quantitatively: ^{1}H NMR (C_5D_5N, 298 K): $\delta = 8.24$ (d, $J = 8.3$ Hz, 4H; arom), 7.16 (m, 12H; arom), 5.13 (d, $J = 11.2$ Hz, 4H; CH_2-calix), 4.02 (br s, 3H; CH_3N), 3.21 (d, $J = 11.2$ Hz, 4H; CH_2-calix), 2.26 (s, 6H; CH_3-*p*-tol), 2.17 (s, 9H; *t*BuN), 1.12 (s, 36H; *t*Bu); ^{13}C NMR (C_5D_5N, 298 K): $\delta = 156.93$ (arom-quat), 148.53 (arom-quat), 140.98 (arom-quat), 132.85 (arom-quat), 130.27 (CH-*p*-tol), 127.60 (CH-*p*-tol), 124.26 (CH-arom), 77.75 (CN-quat), 63.84 (CN-quat),47.74 (NCH_3), 34.51 (*t*Bu-quat), 33.82 (CH_2-calix), 33.35 (CH_3-*t*BuNC), 31.78 (CH_3-*t*Bu-calix), 20.95 (CH_3-*p*-tol).

Synthesis of 19: Pyridine (20 mL) was added to a yellow solution of **16** · C_6H_6 (0.97 g, 0.81 mmol) in toluene (60 mL). After 36 h volatiles were removed in a vacuum and the solid residue was washed with pentane (50 mL) and collected. Yield: 0.601 g (63%); ^{1}H NMR (C_5D_5N, 298 K): $\delta = 8.19$ (br d, $J = 6.34$ Hz, 2H; arom), 7.98 (br s, 2H; arom), 7.91 (d, $J = 7.32$ Hz, 4H; arom), 7.38 (m, 3H; arom), 7.21 (s, 8H; arom-calix), 7.18 (m, 4H; arom), 5.22 (d, $J = 11.22$ Hz, 4H; CH_2-calix), 4.83 (d, $J = 15.62$ Hz, 2H; CH_2Ph), 4.50 (d, $J = 15.62$ Hz, 2H; CH_2Ph), 3.50 (br s, 3H; CH_3-N), 3.33 (d, $J = 11.22$ Hz, 4H; CH_2-calix), 1.95 (s, 9H; *t*BuNC), 1.16 (s, 36H; *t*Bu-calix); ^{1}H NMR (C_6D_6, 298 K): $\delta = 7.72$ (d, $J = 7.32$ Hz, 4H; arom), 7.06 (m, 6H; arom), 6.92 (s, 8H; arom-calix), 6.41 (br s, 1H; pyridine),6.05 (br s, 2H; pyridine), 5.85 (br s, 2H; pyridine), 5.06 (d, $J = 12.68$ Hz, 4H; CH_2-calix), 4.88 (d, $J = 16.1$ Hz, 2H; CH_2Ph), 4.41 (d, $J = 16.1$ Hz, 2H; CH_2Ph), 3.13 (d, $J = 12.68$ Hz, 4H; CH_2-calix), 2.01 (s, 9H; *t*BuNC), 1.64 (br s, 3H; CH_3-N) 1.03 (s, 36H; *t*Bu-calix); anal. calcd for $C_{69}H_{83}N_2O_4Ta$ (1185.38): C 69.92, H 7.06, N 2.36; found: C 66.18, H 7.41, N 2.21.

Synthesis of 20: Pyridine (20 mL) was added to a yellow solution of **17** (0.95 g, 0.85 mmol) in toluene (60 mL). After 24 h volatiles were removed in a vacuum and the solid residue was washed with *n*-hexane (60 mL) and collected. Yield: 0.75 g (75%); ^{1}H NMR (C_5D_5N, 298 K): $\delta = 8.56$ (br s, 2H; pyridine), 8.24 (d, $J = 8.28$ Hz, 4H; *p*-tol), 8.03 (br s, 1H; pyridine), 7.34 (br t, 2H; pyridine), 7.14 (d, $J = 8.28$ Hz, 4H; *p*-tol), 7.12 (s, 8H; arom-calix), 5.12 (d, $J = 11.24$ Hz, 4H; CH_2-calix), 3.94 (br s, 3H; CH_3-N), 3.21 (d, $J = 11.24$ Hz, 4H; CH_2-calix), 2.26 (s, 6H; CH_3-*p*-tol), 2.17 (s, 9H; *t*BuNC), 1.12 (s, 36H; *t*Bu-calix); anal. calcd for $C_{69}H_{83}N_2O_4Ta$ (1185.38): C 69.92, H 7.06, N 2.36; found: C 68.04, H 7.29, N 2.10.

Synthesis of 21: A solution of LiC≡CPh (1.20 g, 11.15 mmol) in THF (20 mL) was added dropwise to a stirred yellow solution of **4** · C_7H_8 (5.60 g, 5.58 mmol) in toluene (100 mL). After 12 h a black suspension was observed. Volatiles were removed in a vacuum and the residue extracted with diethyl ether (120 mL). The solvent was evaporated to dryness, the residue washed with *n*-hexane (70 mL), and collected as a yellow microcrystalline solid. Yield: 3.33 g (42%). Crystals suitable for X-ray analysis were grown from a saturated diethyl ether solution at room temperature. ^{1}H NMR (C_6D_6, 298 K): $\delta = 8.97$ (d, $J = 7.6$ Hz, 4H; arom), 7.23 (m, 19H; arom), 5.18 (d, $J = 13.8$ Hz, 1H; CH_2-calix), 5.16 (d, $J = 13.18$ Hz, 1H; CH_2-calix), 4.71 (d, $J = 13.8$ Hz, 1H; CH_2-calix), 4.59 (d, $J = 14.0$, 1H; CH_2-calix), 3.76 (s, 3H; OCH_3), 3.51 (d, $J = 13.8$ Hz, 1H; CH_2-calix), 3.47 (d, $J = 13.8$ Hz, 1H; CH_2-calix), 3.34 (d, $J = 13.8$ Hz, 1H; CH_2-calix), 3.16 (d, $J = 14.0$ Hz, 1H; CH_2-calix), 2.34 (br s, 8H; Et_2O), 1.48 (s, 9H; *t*Bu), 1.35 (s, 9H; *t*Bu), 1.07 (s, 9H; *t*Bu), 1.03 (s, 9H; *t*Bu), 0.62 (br s, 12H; Et_2O); IR (Nujol): $\tilde{\nu} = 2087$ cm^{-1}; anal. calcd. for **21** · 2 Et_2O, $C_{77}H_{90}O_6Ta$ (1292.51): C 71.55, H 7.02, found: C 70.86, H 6.97. Complex **22** is formed, regardless of the Ta/LiC≡CPh stoichiometry employed (i.e. 1:2.)

0947-6539/99/0502-0734 $ 17.50+.50/0 *Chem. Eur. J.* **1999**, *5*, No. 2

Synthesis of 22: A solution of (CH_2=CH-CH_2)MgCl (0.58 M, 12.93 mmol) in THF (22.29 mL) was added dropwise to a yellow solution of **4**·C_7H_8 (6.49 g, 6.46 mmol) in THF (120 mL) at −10 °C. The mixture became orange in seconds. After 2 h dioxane (3 mL) was added. Volatiles were removed in a vacuum and the solid residue was extracted with diethyl ether (300 mL). The solvent was evaporated to dryness, the very soluble residue was washed with benzene (80 mL), and collected as a yellow powder. Yield: 2.2 g (34 %); ^{1}H NMR (C_6D_6, 298 K): δ = 7.26 (d, J = 2.42 Hz, 2H; arom), 7.23 (d, J = 2.42 Hz, 2H; arom), 7.15 (s, 6H; benzene), 6.94 (qt, J = 10.74 Hz, 2H; CH-allyl), 6.82 (s, 4H; arom), 5.02 (d, J = 12.7 Hz, 2H; CH_2-calix), 4.46 (d, J = 12.7 Hz, 2H; CH_2-calix), 4.06 (d, J = 10.74 Hz, 8H; CH_2-allyl), 3.71 (s, 3H; OCH_3), 3.35 (d, J = 12.7 Hz, 2H; CH_2-calix), 3.22 (d, J = 12.7 Hz, 2H; CH_2-calix), 1.39 (s, 18H; *t*Bu), 0.78 (s, 9H; *t*Bu), 0.70 (s, 9H; *t*Bu); anal. calcd. for **22**·C_6H_6, $C_{57}H_{71}O_4Ta$ (1001.14): C 68.38, H 7.15; found: C 68.67, H 7.20. The ^{1}H NMR spectrum of **22** in C_7D_8 at −80 °C did not show any significant changes.

Synthesis of 23: A solution of (CH_2=CH-CH_2)MgCl (0.58 M, 9.49 mmol) in THF (16.36 mL) was added dropwise to a yellow solution of **4**·C_7H_8 (4.76 g, 4.74 mmol) in benzene (120 mL). The mixture turned orange within seconds. After 3 h dioxane (3 mL) was added. Volatiles were removed in a vacuum and *n*-hexane (40 mL) and diethyl ether (40 mL) were added to the residue. The salts were filtered off and the resulting solution was saturated with CO. The mixture turned light orange within seconds and was then kept at −30 °C for 48 h to yield a white precipitate. Yield: 2.07 g (46 %); ^{1}H NMR (C_6D_6, 298 K): δ = 7.24 (d, J = 2.2 Hz, 2H; arom), 7.15 (d, J = 2.2 Hz, 2H; arom), 6.87 (s, 2H; arom), 6.81 (s, 2H; arom), 6.65 (m, 2H; CH-allyl), 5.38 (dd, J = 17.2 Hz, J = 2 Hz, 2H; CH_2-vinyl), 5.27 (dd, J = 10 Hz, J = 2 Hz, 2H; CH_2-vinyl), 4.96 (d, J = 12.4 Hz, 2H; CH_2-calix), 4.31 (s, 3H; OCH_3), 4.19 (d, J = 12.4 Hz, 2H; CH_2-calix), 3.97 (dd, J = 14.8 Hz, J = 8 Hz, 2H; CH_2-allyl), 3.66 (dd, J = 14.8 Hz, J = 6.4 Hz, 2H; CH_2-allyl), 3.25 (d, J = 12.4 Hz, 2H; CH_2-calix), 3.10 (d, J = 12.4 Hz, 2H; CH_2-calix), 1.38 (s, 18H; *t*Bu), 0.85 (s, 9H; *t*Bu), 0.68 (s, 9H; *t*Bu); anal. calcd for $C_{52}H_{65}O_5Ta$ (951.03): C 65.67, H 6.89; found: C 65.60, H 6.75.

Synthesis of 24: A solution of CH_2=$CHCH_2MgCl$ (0.7 M, 7.50 mmol) in THF (10.72 mL) was added dropwise to a yellow solution of **4**·C_7H_8 (3.77 g, 3.75 mmol) in THF (200 mL). The mixture turned orange within seconds. After 8 h dioxane (3 mL) was added. Volatiles were removed in a vacuum and benzene was added to the orange residue. Salts were filtered off and *t*BuNC (0.31 g, 1.7 mmol) was added to the solution. The mixture turned to red in seconds. After 12 h the volatiles were removed in a vacuum, the solid residue was washed with pentane (60 mL), and a very light orange powder was collected. Yield: 1.4 g (38 %); ^{1}H NMR (C_6D_6, 298 K): δ = 7.32 (s, 4H; arom), 6.87 (s, 2H; arom), 6.82 (s, 2H; arom), 6.28 (m, 2H; CH-allyl), 5.16 (dd, J = 17.32 Hz, J = 2.44 Hz; 2H; CH_2 vinyl), 5.06 (dd, J = 9.76 Hz, J = 2.44 Hz, 2H; CH_2-vinyl), 4.98 (d, J = 12.4 Hz, 2H; CH_2-calix), 4.52 (d, J = 12.4 Hz, 2H; CH_2-calix), 4.24 (s, 3H; OCH_3), 3.79 (dd, J = 14.9 Hz, J = 6.4 Hz, 2H; CH_2-allyl), 3.31 (dd, J = 14.9 Hz, J = 8.0 Hz, 2H; CH_2-allyl), 3.26 (d, J = 12.4 Hz, 2H; CH_2-calix), 3.25 (d, J = 12.4 Hz, 2H; CH_2-calix), 1.93 (s, 9H; *t*BuN), 1.40 (s, 18H; *t*Bu), 0.86 (s, 9H; *t*Bu), 0.70 (s, 9H; *t*Bu); anal. calcd for $C_{56}H_{74}NO_4Ta$ (1006.16): C 66.85, H 7.41, N 1.39; found: C 65.72, H 7.71 N 1.36.

Synthesis of 25: [Mg(C_4H_6)·thf_2] (13.18 g, 14.14 mmol) was added to a yellow solution of **4**·C_7H_8 (14.20 g, 14.14 mmol) in benzene (250 mL) at room temperature. The mixture became red in seconds. The mixture was stirred for 2 h, then dioxane (5 mL) was added to the suspension that was extracted with benzene. Volatiles were removed in a vacuum and the orange residue was washed with *n*-hexane (80 mL), collected, and dried in a vacuum. Yield: 9.5 g (71 %); ^{1}H NMR (C_6D_6, 298 K): δ = 7.26 (d, J = 2.44 Hz, 2H; arom), 7.22 (d, J = 2.44 Hz, 2H; arom), 7.05 (m, 2.5H; tol), 6.87 (s, 2H; arom), 6.82 (s, 2H; arom), 6.45 (m, 2H; CH-butadiene), 4.54 (d, J = 12.7 Hz, 2H; CH_2-calix), 4.22 (d, J = 12.2 Hz, 2H; CH_2-calix), 3.99 (s, 3H; OCH_3), 3.28 (d, J = 12.7 Hz, 2H; CH_2-calix), 3.18 (d, J = 12.2 Hz, 2H; CH_2-calix), 2.69 (d, J = 7.32 Hz, 4H; CH_2-butadiene), 2.1 (s, 1.5H; CH_3-toluene), 1.41 (s, 18H; *t*Bu), 0.82 (s, 9H; *t*Bu), 0.72 (s, 9H; *t*Bu); ^{13}C NMR (decoupled) (C_7H_8, 298 K): δ = 159.6 (arom-quat), 157.0 (arom-quat), 154.1 (arom-quat), 148.9 (arom-quat), 144.1 (arom-quat), 143.1 (arom-quat), 132.3 (arom-quat), 132.1 (arom-quat), 130.1 (arom-quat), 128.5 (arom-quat), 127.3 (CH-arom), 126.0 (CH-butadiene), 125.8 (CH-arom), 125.2 (CH-arom), 123.7 (CH-arom), 67.9 (-OCH_3), 66.8 (CH_2-butadiene), 34.4 (*t*Bu-quat), 34.2 (CH_2-calix), 33.8 (CH_2-calix), 33.4 (*t*Bu-quat), 32.0 (CH_3-*t*Bu-calix), 31.1 (CH_3-*t*Bu-calix), 30.6 (CH_3-*t*Bu-calix); ^{13}C NMR (coupled) (C_7D_8, 298 K): δ = 67.9 (q, J = 146.7 Hz, OCH_3), 66.8 (br t, J = 151 Hz; CH_2-butadiene); anal. calcd for **25**·0.5C_7H_8, $C_{52.5}H_{65}O_4Ta$ (941.04): C 67.01, H 6.96; found: C 66.97, H 7.08.

Synthesis of 26: A solution of *t*BuNC (0.27 g, 3.28 mmol) in toluene (20 mL) was added dropwise to a stirred solution of **25**·0.5C_7H_8 (1.54 g, 1.64 mmol) in toluene (100 mL). The mixture was stirred for 7 days. The solvent was removed in a vacuum and the orange residue washed with *n*-hexane (50 mL) and collected as a white powder. Yield: 1.00 g (63 %); ^{1}H NMR (C_6D_6, 298 K): δ = 7.23 (d, J = 2.44 Hz, 2H; arom), 7.21 (d, J = 2.44 Hz, 2H; arom), 6.87 (s, 2H; arom), 6.82 (s, 2H; arom), 6.05 (s, 2H; CH-butadiene.), 4.97 (d, J = 12.7 Hz, 2H; CH_2-calix), 4.35 (d, J = 12.2 Hz, 2H; CH_2-calix), 4.17 (s, 3H; OCH_3), 3.78 (d, J = 15.6 Hz, 2H; CH_2-butadiene), 3.26 (d, J = 12.7 Hz, 2H; CH_2-calix), 3.21 (d, J = 12.2 Hz, 2H; CH_2-calix), 3.16 (d, J = 15.6 Hz, 2H; CH_2-butadiene), 1.99 (s, 9H; *t*BuN), 1.40 (s, 18H; *t*Bu), 0.85 (s, 9H; *t*Bu), 0.69 (s, 9H; *t*Bu); ^{13}C NMR (C_6D_6, 298 K): δ = 156.12 (arom-quat), 153.06 (arom-quat), 150.33 (arom-quat), 149.97 (arom-quat), 144.67 (arom-quat), 142.56 (arom-quat), 133.40 (CH-butadiene), 132.66 (arom-quat), 132.41 (arom-quat), 130.47 (arom-quat), 130.17(arom-quat), 127.43 (CH-arom), 125.58 (CH-arom), 125.32 (CH-arom), 123.43 (CH-arom),74.43 (CN-quat), 72.05 (-OCH_3), 63.04 (CN-quat), 45.84 (CH_2-butadiene), 34.31 (*t*Bu-quat), 33.81 (*t*Bu-quat), 33.49 (*t*Bu-quat), 33.40 (CH_3-*t*BuNC), 33.31 (CH_2-calix), 33.27 (CH_2-calix), 31.95 (CH_3-*t*Bu-calix), 31.17 (CH_3-*t*Bu-calix), 30.55 (CH_3-*t*Bu-calix); anal. calcd for $C_{54}H_{70}NO_4Ta$ (978.10): C 66.31, H 7.21, N 1.43; found: C 65.67, H 7.64, N 1.25.

Synthesis of 27: $(CH_3)_2CO$ (0.136 g, 2.34 mmol) was added to a solution of **25**·0.5C_7H_8 (1.1 g, 1.17 mmol) in benzene (120 mL). The orange solution immediately turned light yellow. The solution was filtered, the solvent evaporated to dryness, the white residue washed with *n*-hexane (30 mL) and then collected. Yield: 0.9 g (76 %). Crystals suitable for X-ray analysis were grown from a saturated solution in THF and *n*-hexane at room temperature. ^{1}H NMR (C_6D_6, 298 K): δ = 7.40 (d, J = 1.96 Hz, 2H; arom), 7.35 (d, J = 1.96 Hz, 2H; arom), 7.06 (s, 2H; arom), 7.03 (s, 2H; arom), 5.69 (m, 2H; CH-butadiene), 5.05 (d, J = 13.16 Hz, 2H; CH_2-calix), 4.31 (d, J = 13.18 Hz, 2H; CH_2-calix), 3.86 (s, 3H; OCH_3), 3.59 (d, J = 13.16 Hz, 2H; CH_2-calix), 3.48 (d, J = 13.18 Hz, 2H; CH_2-calix), 2.45 (br s, 2H; butadiene), 2.08 (br s, 2H; butadiene),1.42 (s, 18H; *t*Bu), 1.34 (s, 6H; Me-acetone), 1.09 (s, 6H; Me-acetone), 0.84 (s, 9H; *t*Bu), 0.75 (s, 9H; *t*Bu); anal. calcd for $C_{55}H_{73}O_6Ta$ (1011.13): C 65.33, H 7.28; found: C 65.70, H 7.48.

Synthesis of 28: PhN_3 (0.59 g, 4.94 mmol) was added to a solution of **25**·0.5C_7H_8 (1.54 g, 1.64 mmol) in THF (120 mL). After 7 days the orange solution was filtered. The solvent was evaporated to dryness, the white residue washed with *n*-hexane (50 mL), and then collected. Yield: 1.00 g (63 %). Crystals suitable for X-ray analysis were grown in a saturated solution in toluene/pentane at 4 °C. ^{1}H NMR (C_6D_6, 298 K): δ = 7.49 (d, J = 7.32 Hz, 2H; arom), 7.02 (m, 12.5H; arom), 6.38 (t, J = 7.32 Hz, 1H; arom), 4.96 (s, 3H; OCH_3), 4.91 (d, J = 13.18 Hz, 2H; CH_2-calix), 4.54 (d, J = 12.4 Hz, 2H; CH_2-calix), 3.32 (d, J = 13.18 Hz, 2H; CH_2-calix), 3.28 (d, J = 12.4 Hz, 2H; CH_2-calix), 2.1 (s, 1.5H; CH_3-tol), 1.35 (s, 18H; *t*Bu), 0.78 (s, 9H; *t*Bu), 0.67 (s, 9H; *t*Bu); anal. calcd for **28**·C_7H_8, $C_{109}H_{128}N_2O_8Ta_2$ (1956.12): C 66.93, H 6.60, N 1.43; found: C 66.94, H 6.90, N 1.26.

X-ray crystallography of complexes 4, 8a, 13, 19, and 28: Suitable crystals were mounted in glass capillaries and sealed under nitrogen. Reduced cells were obtained with the use of TRACER.[23] Data were collected on a single-crystal diffractometer (Siemens AED for **4** and Rigaku AFC6S for **8a**, **13**, **19**, and **28**) at 295 K for **4** and at 133 K for **8a**, **13**, **19**, and **28**. The individual reflection profiles were analyzed for intensities and background.[24] The structure amplitudes were obtained after the usual Lorentz and polarization[25] corrections, and the absolute scale was established by the Wilson method.[26] For all complexes the crystal quality was tested by ψ-scans which showed that crystal absorption effects could not be neglected. Data were then corrected for absorption with the program ABSORB[27] for **4** and a semiempirical method[28] for **8a**, **13**, **19**, and **28**. The function minimized during the full-matrix least-square refinements was $\Sigma w(\Delta F^2)^2$. Anomalous scattering corrections were included in all calculations of the structural factors.[29b] Scattering factors for neutral atoms were taken from ref. [29a] for non-hydrogen atoms and from ref. [30] for H. Structure solutions[31] were based on the observed reflections [$I > 2\sigma(I)$] while the refinements were based on the unique reflections with $I > 0$. The structures

were solved by the heavy-atom method starting from a three-dimensional Patterson map. Refinements were performed by full-matrix least-squares, first isotropically and then anisotropically for all non-H atoms, except for the disordered atoms. For all complexes, the hydrogen atoms were placed in geometrically calculated positions and introduced into the refinements as fixed atom contributions ($U_{iso} = 0.12$, 0.05, 0.05, 0.05, and 0.06 Å^2 for **4**, **8a**, **13**, **19**, and **28**, respectively). The H atoms associated with the disordered carbon atoms were ignored. In the last stage of refinement the weighting scheme $w = 1/[\sigma^2(F_o^2) + (aP)^2]$ (with $P = (F_o^2 + 2F_c^2)/3$ was applied which gave $a = 0.1700$, 0.1101, 0.1306, 0.0994, and 0.1342 for **4**, **8a**, **13**, **19**, and **28**, respectively. All calculations were performed by with SHELX93.[32] The final difference map for complex **4** showed a residual peak of 1.27 e Å^{-3} near the metal atom in the direction of the Ta–O(2) bond (general background 0.52 e Å^{-3}). For complex **8a**, four residual peaks, which range from 3.64 to 1.61 e Å^{-3}, were found in the proximity of the metal atom along with the Ta–O bonds (general background 0.61 e Å^{-3}). In complex **13**, two residual peaks of 1.79 and 1.74 e Å^{-3} were found in the proximity of the metal atom in the direction of the Ta–O(4) and Ta–O(2) bonds (general background 0.75 e Å^{-3}). In complex **19**, two residual peaks of 2.33 and 1.76 e Å^{-3} were found in the proximity of the metal atom in the direction of the Ta–O(3) and Ta–O(1) bonds (general background 0.52 e Å^{-3}). In complex **28**, two residual peaks of 5.20 and 5.00 e Å^{-3} were found in the proximity of the metal atom in the direction of the Ta–N(1) and Ta–O(1) bonds (general background 0.65 e Å^{-3}).

*Complex **4***: All the methyl carbon atoms of the *t*Bu groups were affected by high thermal parameters which indicates the presence of disorder. The best fit was obtained by splitting the atoms over two positions (A and B), and isotropically refined with a site occupation factor of 0.5. The C–C bond lengths within the disordered *t*Bu groups were constrained to be 1.54(1) Å. The guest toluene solvent molecule (C(51)–C(57)) was found to be statistically distributed over two positions (A and B) and isotropically refined with a site occupation factor of 0.5.

*Complex **8a***: All but one out of the five and a half crystallographically independent pyridine solvent molecules of crystallization were affected by severe disorder. This was solved by splitting the atoms over two positions (A and B), and isotropically refined with site occupation factors of 0.5. The nitrogen atom of three molecules could not be unambiguously determined. During the refinement the disordered pyridine rings were constrained to have a D_{6h} symmetry.

*Complex **13***: The C(35) and C(36) methyl carbon atoms of a *t*Bu group were affected by high thermal parameters which indicates the presence of disorder. The best fit was found by splitting the atoms over two positions (A and B), and isotropically refined with site occupation factors of 0.5.

*Complex **19***: The C(30) and C(31) methyl carbon atoms of a *tert*-butyl group reached rather high thermal parameters, so they were split over two positions (A and B), and isotropically refined with site occupation factors of 0.7 and 0.3, respectively. The methylpyridinium cation, the diethyl ether solvent molecule, and two of the benzene solvent molecules were affected by severe disorder. This was solved by splitting the atoms over two positions (A and B). The C–C and C–O bond lengths within the disordered Et_2O molecule were constrained to be 1.54(1) and 1.44(1) Å, respectively. During the refinement the disordered aromatic rings were constrained to have a D_{6h} symmetry.

*Complex **28***: Some methyl carbon atoms of two *t*Bu were affected by disorder, which was solved by splitting the atoms over two positions (A and B), and isotropically refined with site occupation factors of 0.75 and 0.25, respectively, for C(30)–C(32), and of 0.5 for the A and B positions of C(38)–C(40). Moreover, the toluene solvent molecule of crystallization showed rather high thermal parameters, which indicates the presence of disorder. The best fit was obtained by splitting the C(72) and C(73) atoms over two positions (A and B), and isotropically refined with site occupation factors of 0.6 and 0.4, respectively.

Crystallographic data (excluding structure factors) for the structures reported in this paper have been deposited with the Cambridge Crystallographic Data Centre as supplementary publication nos. CCDC-102934 (**4**), 102935 (**7a**), 102936 (**8a**), 102937 (**13**), 102938 (**19**), 102939 (**21**), and 102940 (**28**). Copies of the data can be obtained free of charge on application to CCDC, 12 Union Road, Cambridge CB2 1EZ, UK (fax: (+44) 1223-336-033; e-mail: deposit@ccdc.cam.ac.uk).

Acknowledgments

We thank the Fonds National Suisse de la Recherche Scientifique (Bern, Switzerland, Grant No. 20-53′336.98), Ciba Specialty Chemicals (Basel, Switzerland), and Fondation Herbette (University of Lausanne, N.R.) for financial support.

[1] C. D. Gutsche, *Calixarenes*, Royal Society of Chemistry, Cambridge **1989**; *Calixarenes, A Versatile Class of Macrocyclic Compounds* (Eds.: J. Vicens, V. Böhmer), Kluwer, Dordrecht, **1991**; V. Bohmer, *Angew. Chem.* **1995**, *107*, 785–817; *Angew. Chem. Int. Ed. Engl.* **1995**, *34*, 713–745.

[2] a) L. Giannini, E. Solari, A. Zanotti-Gerosa, C. Floriani, A. Chiesi-Villa, C. Rizzoli, *Angew. Chem.* **1996**, *108*, 79–82; *Angew. Chem. Int. Ed. Engl.* **1996**, *35*, 85–87; b) L. Giannini, E. Solari, A. Zanotti-Gerosa, C. Floriani, A. Chiesi-Villa, C. Rizzoli, *Angew. Chem.* **1996**, *108*, 3051–3053; *Angew. Chem. Int. Ed. Engl.* **1996**, *35*, 2825–2827; c) *Angew. Chem.* **1997**, *109*, 763–765; *Angew. Chem. Int. Ed. Engl.* **1997**, *36*, 753–754; d) L. Giannini, A. Caselli, E. Solari, C. Floriani, A. Chiesi-Villa, C. Rizzoli, N. Re, A. Sgamellotti, *J. Am. Chem. Soc.* **1997**, *119*, 9198–9210; e) L. Giannini, A. Caselli, E. Solari, C. Floriani, A. Chiesi-Villa, C. Rizzoli, N. Re, A. Sgamellotti, *J. Am. Chem. Soc.* **1997**, *119*, 9709–9719; f) M. Giusti, E. Solari, L. Giannini, C. Floriani, A. Chiesi-Villa, C. Rizzoli, *Organometallics* **1997**, *16*, 5610–5612; g) A. Zanotti-Gerosa, E. Solari, L. Giannini, C. Floriani, A. Chiesi-Villa, C. Rizzoli, *J. Am. Chem. Soc.* **1998**, *120*, 437–438; h) L. Giannini, E. Solari, C. Floriani, A. Chiesi-Villa, C. Rizzoli, *J. Am. Chem. Soc.* **1998**, *120*, 823–824; i) A. Zanotti-Gerosa, E. Solari, L. Giannini, C. Floriani, N. Re, A. Chiesi-Villa, C. Rizzoli, *Inorg. Chim. Acta* **1998**, *270*, 298–311; j) M. G. Gardiner, S. M. Lawrence, C. L. Raston, B. W. Skelton, A. H. White, *Chem. Commun.* **1996**, 2491–2492; k) M. G. Gardiner, G. A. Koutsantonis, S. M. Lawrence, P. J. Nichols, C. L. Raston, *Chem. Commun.* **1996**, 2035–2036; l) V. C. Gibson, C. Redshaw, W. Clegg, M. R. J. Elsegood, *J. Chem. Soc. Chem. Commun.* **1995**, 2371–2372; m) J. A. Acho, L. H. Doerrer, S. J. Lippard, *Inorg. Chem.* **1995**, *34*, 2542–2556.

[3] a) E.-I. Negishi, T. Takahashi, *Acc. Chem. Res.* **1994**, *27*, 124–130 and references therein; b) M. T. Reetz in *Organometallics in Synthesis* (Ed.: M. Schlosser), Wiley, New York, **1994**, Ch. 3; c) G. Erker, R. Pfaff, *Organometallics* **1993**, *12*, 1921–1926; d) E.-I. Negishi in *Comprehensive Organic Synthesis, Vol. 5* (Ed.: L. A. Paquette), Pergamon, Oxford, **1991**, pp. 1163–1184; e) N. E. Schore in ref. [3d], pp. 1037–1064; f) S. L. Buchwald, R. B. Nielsen, *Chem. Rev.* **1988**, *88*, 1047–1058.

[4] B. C. Parkin, J. R. Clark, V. M. Visciglio, P. E. Fanwick, I. P. Rothwell, *Organometallics* **1995**, *14*, 3002–3013; J. R. Clark, P. E. Fanwick, I. P. Rothwell, *J. Chem. Soc. Chem. Commun.* **1995**, 553–554; J. S. Yu, B. C. Ankianiec, M. T. Nguyen, I. P. Rothwell, *J. Am. Chem. Soc.* **1992**, *114*, 1927–1929; R. W. Chesnut, G. G. Jacob, J. S. Yu, P. E. Fanwick, I. P. Rothwell, *Organometallics* **1991**, *10*, 321–328.

[5] J. B. Bonanno, P. T. Wolczanski, E. B. Lobkovsky, *J. Am. Chem. Soc.* **1994**, *116*, 11159–11160; R. L. Miller, R. Toreki, R. E. LaPointe, P. T. Wolczanski, G. D. Van Duyne, D. C. Roe, *J. Am. Chem. Soc.* **1993**, *115*, 5570–5588.

[6] B. Castellano, A. Zanotti-Gerosa, E. Solari, C. Floriani, A. Chiesi-Villa, C. Rizzoli, *Organometallics* **1996**, *15*, 4894–4896.

[7] a) F. Corazza, C. Floriani, A. Chiesi-Villa, C. Guastini, *J. Chem. Soc. Chem. Commun.* **1990**, 1083–1084; b) A. Zanotti-Gerosa, E. Solari, L. Giannini, C. Floriani, A. Chiesi-Villa, C. Rizzoli, *Chem. Commun.* **1997**, 183–184.

[8] L. D. Durfee, I. P. Rothwell, *Chem. Rev.* **1988**, *88*, 1059–1079.

[9] L. R. Chamberlain, B. D. Steffey, I. P. Rothwell, J. C. Huffman, *Polyhedron* **1989**, *8*, 341–349; L. R. Chamberlain, L. D. Durfee, P. E. Fanwick, L. M. Kobriger, S. L. Latesky, A. K. McMullen, B. D. Steffey, I. P. Rothwell, K. Folting, J. C. Huffman, *J. Am. Chem. Soc.* **1987**, *109*, 6068–6076.

[10] C. Floriani, N. Re, unpublished results.

[11] The benzene guest molecule (C(71)–C(76)) enters the cavity of the complex molecule with its C(71)–C(74) axis oriented parallel to the axis of the calixarene molecule, as indicated by the value of the Ta-

0947-6539/99/0502-0736 $ 17.50+.50/0 *Chem. Eur. J.* **1999**, *5*, No. 2

C(71)-(74) angle [176.9(10)°]. The Ta ··· C(71) distance of 4.909(12) Å rules out any possible Ta ··· H interaction. The guest molecule is oriented to be nearly parallel to the B and D rings [dihedral angles 23.6(4) and 23.3(4)° respectively] and perpendicular to the A and C rings [dihedral angles 89.8(4) and 86.3(3)° respectively]. In spite of the disorder involving some *t*Bu groups, the host–guest interactions could be interpreted in terms of CH_3/π-interactions occurring between the protons of the methyl groups of the B and D rings of the host and the guest aromatic ring, as suggested by the contact distances: C(36)B ··· C(71) = 3.96(3), C(36)B ··· C(74) = 3.84(3), C(36)B ··· C(72) = 3.59(3), C(43 ··· C(73) = 3.93(4), C(36)B ··· C(73) = 3.48(3) Å.

[12] S. U. Koschmieder, B. Hussain-Bates, M. B. Hursthouse, G. Wilkinson, *J. Chem. Soc. Dalton Trans.* **1991**, 2785–2790; M. V. Galakhov, M. Gomez, G. Jimenez, P. Royo, M. A. Pellinghelli, A. Tiripicchio, *Organometallics* **1995**, *14*, 1901–1910; S. D. Gray, K. J. Weller, M. A. Bruck, P. M. Briggs, D. E. Wigley, *J. Am. Chem. Soc.* **1995**, *117*, 10678–10693.

[13] a) D. E. Wigley, S. D. Gray, in *Comprehensive Organometallic Chemistry II*, *Vol. 5* (Eds.: E. W. Abel, F. G. A. Stone, G. Wilkinson), Pergamon, Oxford, **1995**, Ch. 2; b) T. Okamoto, H. Yasuda, A. Nakamura, Y. Kai, N. Kanehisa, N. Kasai, *Organometallics* **1988**, *7*, 2266–2273; c) K. Mashima, S. Fujikawa, Y. Tanaka, H. Urata, T. Oshiki, E. Tanaka, A. Nakamura, *Organometallics* **1995**, *14*, 2633–2640; d) K. Mashima, Y. Tanaka, M. Kaidzu, A. Nakamura, *Organometallics* **1996**, *15*, 2431–2433.

[14] A. Caselli, L. Giannini, E. Solari, C. Floriani, N. Re, A. Chiesi-Villa, C. Rizzoli, *Organometallics* **1997**, *16*, 5457–5469 and references therein.

[15] In this orientation the C(67) methyl group of toluene extends towards ring C; the separation between C(67) and the C(15)–C(20) aromatic carbon atoms of the ring C ranges from 3.721(20) to 3.895(20) Å. The host–guest interactions could be interpreted in terms of CH_3/π interactions occurring between the protons of the methyl groups of the rings B and D of the host and the guest aromatic ring. In particular, two opposite protons from the C(34) and C(42) methyl groups are oriented to point towards the center of gravity of the toluene ring, as suggested by the contact distances listed below (C_b refers to the center of gravity of the toluene ring): $C_b \cdots C(34) = 3.781(19)$, $C_b \cdots H(341) = 2.78$; $C_b \cdots C(42) = 3.896(17)$, $C_b \cdots H(422) = 2.91$ Å.

[16] W. A. Nugent, J. M. Mayer, *Metal–Ligand Multiple Bonds*, Wiley, New York, **1988**, Ch. 5, p. 180.

[17] a) R. Hoffmann, W. N. Lipscomb, *J. Chem. Phys.* **1962**, *36*, 2179; b) R. Hoffmann, *J. Chem. Phys.* **1963**, *39*, 1397.

[18] a) K. Tatsumi, A. Nakamura, P. Hofmann, P. Stauffert, R. Hoffmann, *J. Am. Chem. Soc.* **1985**, *107*, 4440–4451; b) P. Hofmann, P. Stauffert, K. Tatsumi, A. Nakamura, R. Hoffmann, *Organometallics* **1985**, *4*, 404–406.

[19] K. Tatsumi, H. Yasuda, A.Nakamura, *Isr. J. Chem.* **1983**, *23*, 145–150.

[20] a) H. Yasuda, K. Tatsumi, A. Nakamura, *Acc. Chem. Rev.* **1985**, *18*, 120–126; b) G. Erker, C. Kruger, G. Muller, *Adv. Organomet. Chem.* **1985**, *24*, 1–39; c) J. Blenkers, B. Hessen, F. van Bolhuis, A. J. Wagner, J. H. Teuben, *Organometallics* **1987**, *6*, 459–469; d) H. Yasuda, K. Tatsumi, T. Okamoto, K. Mashima, K. Lee, A. Nakamura, Y. Kai, N. Kanehisa, N. Kasai, *J. Am. Chem. Soc.* **1985**, *107*, 2410–2422.

[21] M. D. Newton, T. M. Shulmann, M. M. Manus, *J. Am. Chem. Soc.* **1974**, *96*, 17–23.

[22] A. Arduini, A. Casnati, A. in *Macrocycle Synthesis* (Ed.: O. Parker), Oxford University Press, New York, **1996**, Ch. 7.

[23] S. L. Lawton, R. A. Jacobson, *TRACER (a cell reduction program)*, Ames Laboratory, Iowa State University of Science and Technology, Ames, IA, **1965**.

[24] M. S. Lehmann, F. K. Larsen, *Acta Crystallogr. Sect. A: Cryst. Phys. Diffr. Theor. Gen. Crystallogr.* **1974**, *30*, 580–584.

[25] Data reduction, structure solution, and refinement were carried out on an QUANSAN personal computer equipped with an INTEL PENTIUM processor.

[26] A. J. C. Wilson, *Nature* **1942**, *150*, 151.

[27] F. Ugozzoli, *Comput. Chem.* **1987**, *11*, 109.

[28] A. C. T. North, D. C. Phillips, F. S. Mathews, *Acta Crystallogr. Sect. A: Cryst. Phys. Diffr. Theor. Gen. Crystallogr.* **1968**, *24*, 351.

[29] a) *International Tables for X-Ray Crystallography*, Kynoch, Birmingham, **1974**, *Vol. IV*, p. 99; b) Ref. [29a], p. 149.

[30] R. F. Stewart, E. R. Davidson, W. T. Simpson, *J. Chem. Phys.* **1965**, *42*, 3175.

[31] G. M. Sheldrick, SHELX76, program for crystal structure determination, University of Cambridge, **1976**.

[32] G. M. Sheldrick, SHELX93, program for crystal structure refinement, University of Göttingen, **1993**.

Received: June 9, 1998 [F1197]